Journal of African Earth Sciences 106 (2015) 1–16

Contents lists available at ScienceDirect

Journal of African Earth Sciences

journal homepage: www.elsevier.com/locate/jafrearsci

The upper Cenomanian–lower Turonian of the Preafrican Trough (Morocco): Platform configuration and palaeoenvironmental conditions

V. Lebedel [a,*], C. Lézin [b], B. Andreu [b], El M. Ettachfini [c], D. Grosheny [d]

[a] GéHCo, E.A. 6293, Université de Tours, Faculté des sciences et techniques, Parc de Grandmont, 37200 Tours, France
[b] Université de Toulouse, UPS, OMP, GET (Géosciences Environnement Toulouse), CNRS, IRD, 14 Av. E. Belin, 31400 Toulouse, France
[c] Université Chouaïb Doukkali, Faculté des Sciences, Géologie, Laboratoire Géosciences & Techniques de l'Environnement, B.P. 20, 24 000 El Jadida, Morocco
[d] Université de Lorraine, Faculté des sciences, UMR7359 GéoRessource, Département des géosciences, Campus sciences-Aiguillettes, B.P. 70239, 5406 Vandoeuvre-lès-Nancy, France

ARTICLE INFO

Article history:
Received 6 October 2014
Received in revised form 2 March 2015
Accepted 3 March 2015
Available online 17 March 2015

Keywords:
Preafrican Trough (Morocco)
Late Cenomanian–early Turonian
Palaeoenvironmental conditions
Climate
Platform configuration

ABSTRACT

A synthetic study was carried out based on sedimentological, palaeontological, geochemical and mineralogical data of the upper Cenomanian–lower Turonian carbonate platform of the Preafrican Trough (eastern Morocco) in order to (1) propose a 3D representation of the platform and constrain the temporal framework of the dysoxic/anoxic episodes recorded during the OAE2, (2) define and discuss the prevailing climate on the platform during this period, and (3) make comparisons with other Cenomanian–Turonian platforms.

During the late Cenomanian, both before and during the CCIE (Cenomanian Carbon Isotope Excursion), the platform displayed an east–west polarity. Three third-order sequences of transgression–regression can be defined. Dysoxic conditions were developed in the sediments and the bottom waters of the deepest environment (mid- to outer-ramp setting), in the western part of the platform. Well-oxygenated waters were present in the eastern part of the platform (peritidal zone to mid-ramp environment). The climate was arid before the CCIE, becoming warm with contrasted seasons during the CCIE. This climate is associated with a low palaeoproductivity over the entire platform, along with the presence of photozoan followed by heterozoan carbonate-producers, as found also in other parts of the Saharan platform. However, such conditions are not in accordance with many studies which suggest a wet climate during the CCIE, leading to intense chemical weathering of the continent favouring the appearance of high palaeoproductivity at a global scale and the establishment of dysoxic/anoxic conditions. In the Preafrican Trough, poorly-oxygenated waters spread outwards from the deep basins and covered the platform in response to sea-level rise.

Many disturbances are recorded in the platform succession during the early Turonian, after the CCIE. Indeed, just after the C/T boundary, the development of an outer-ramp environment over the entire Preafrican Trough reflects flooding of the platform, linked to the end of the major Cenomanian transgression and the presence of eutrophic conditions which disrupted carbonate-producing organisms. This high palaeoproductivity, due to considerable nutrient input, led to the establishment of highly dysoxic conditions in the bottom and intermediate waters, causing the disappearance of the majority of the Cenomanian palaeontological groups, except for the opportunist benthic and planktonic foraminifera which proliferated. Part of the nutrient input could be due to the presence of a hot and wet climate that may have led a slight increase in the degree of chemical weathering of the continent. Nevertheless, many lines of evidence, such as the decrease of the detrital influx during the early Turonian and the reduction of the weatherable continental areas after the Cenomanian transgression, suggest the existence of another source of nutrient inputs. Combined with the presence of dysoxic/anoxic conditions during the lower Turonian in several regions of the tropical Central Atlantic, the occurrence of these nutrient inputs may be linked to the volcanism/hydrothermalism of the Caribbean LIP and the mid-ocean ridges.

* Corresponding author.
E-mail address: vanessa.lebedel@gmail.com (V. Lebedel).

http://dx.doi.org/10.1016/j.jafrearsci.2015.03.001
1464-343X/

1. Introduction

One of the interesting aspects of mid-Cretaceous times is the occurrence of paleoclimatic, geochemical and palaeontological disturbances during the late Cenomanian–early Turonian (Lüning et al., 2004; Jenkyns, 2010; Flögel et al., 2011; Jarvis et al., 2011; and many others), resulting from the onset of anoxic conditions in the oceanic basins, corresponding to the Oceanic Anoxic Event 2 (OAE2). While this event is generally well recorded and widely studied in oceanic basins owing the deposition and preservation of black shales (Schlanger et al., 1987; Kuhnt et al., 1990), it is poorly expressed in shallow platform environments, where the consequences of anoxia are less well known. However, since these environments are located at the interface between open-ocean and terrestrial realms, their study provides important information on climatic, physical, biological and geochemical processes, coeval with the OAE2, which are not easily detected in pelagic or terrestrial deposits. These processes involve sea-level changes, nutrient and detrital inputs, freshwater influx, changes in oceanic currents (waves, coastal upwellings, etc.), changes in the abundance and diversity of benthic biota, as well as variations in paleodepth and the extension of dysoxic/anoxic waters, etc.

In this study, we are focused in the upper Cenomanian–lower Turonian carbonate platform of the Preafrican Trough (Morocco). This platform, which now forms part of the Saharan platform, was influenced by Tethyan water masses, corresponding to an area extending over Tunisia (Caron et al., 2006; Jati, 2007; Faouzi Zagrarni et al., 2008) and Algeria (Herkat, 1999, 2004; Jati, 2007; Grosheny et al., 2008; Benyoucef et al., 2014; Benyoucef and Meister, 2015), as well as Atlantic water masses recorded in the Essaouira Basin (Andreu, 1991; Ettachfini, 1993; Lüning et al., 2004), Agadir Basin (Andreu, 1989, 1991; Gertsch et al., 2010a; Jati et al., 2010) and Tarfaya Basin (Lüning et al., 2004; Keller et al., 2008) in Morocco. Moreover, the stratigraphic framework of the Preafrican Trough is well established through the studies of Meister and Rhalmi (2002), Ettachfini and Andreu (2004), Ettachfini (2006), Kennedy et al. (2008), Cavin et al. (2010) and Lezin et al. (2012). Previous studies (Ettachfini and Andreu, 2004; Ettachfini, 2006; Lezin et al., 2012; Lebedel et al., 2013; Andreu et al., 2013) show that (1) the positive $\delta^{13}C$ excursion, related to the global extension of dysoxic/anoxic waters during the OAE2, is clearly identifiable on all the studied outcrops, and (2) the platform exhibits an East–West polarity during the late Cenomanian, and becomes flooded during the early Turonian. By comparing sedimentological and palaeontological observations with geochemical data (major, minor and trace elements), Lebedel et al. (2013) show that poorly-oxygenated conditions reached the platform during the late Cenomanian–early Turonian, sometimes associated with an increase of palaeoproductivity.

The aim of the present study is to (1) summarize all the data (from the literature as based on new results) on the upper Cenomanian–lower Turonian of the Preafrican Trough, (2) define and discuss the prevailing climate on the platform during this period and (3) propose a 3D representation of the platform in several key-steps or episodes, including all the data concerning palaeoenvironments, oxygenation, palaeoproductivity, climate, etc. This approach enables us to constrain the timing of the dysoxic/anoxic episodes, the impact of the OAE2 and its consequences on the development of carbonate producers, thus allowing comparisons with other platforms.

2. The upper Cenomanian–lower Turonian of the Preafrican Trough

In this part, we summarize the main available data on the Preafrican Trough and present some new additional results.

2.1. Geographical and geological background

The Preafrican Trough in eastern Morocco belongs to the western part of the extensive Saharan platform. It forms a wide triangular plain between the Moroccan High Atlas and Anti-Atlas mountain ranges (Fig. 1). The sediments of the platform are bounded by the South Atlas fault, which separate it from the Jurassic basins of the High Atlas to the north, the Precambrian and Palaeozoic formations of the Anti-Atlas in the south, and the Tertiary formations of the Hamada du Guir in the east (Fig. 1). The Cretaceous of the Preafrican Trough lies unconformably on a Palaeozoic or Jurassic basement. The Cenomanian–Turonian succession is composed of two Formations (Choubert, 1948; Dubar, 1948; Basse and Choubert, 1959; Choubert and Faure-Muret, 1962; Sereno et al., 1996; Ettachfini and Andreu, 2004; Cavin et al., 2010): (1) the lower and mid Cenomanian lagoonal gypsiferous marls of the Aoufous Formation and (2) a Cenomanian–Turonian escarpment consisting of marine limestones, making up the Akrabou Formation. The studied interval extends from the top of the Aoufous Formation to the top of the Akrabou Formation.

2.2. Biostratigraphy and chemostratigraphy

Three planktonic foraminifera zones are recognized in the Preafrican Trough (Ettachfini and Andreu, 2004; Ettachfini, 2006; Lezin et al., 2012; Lebedel, 2013): the *Rotalipora cushmani* Zone, belonging to the upper Cenomanian, the *Whiteinella archaeocretacea* Zone, in the uppermost Cenomanian–lowermost Turonian, and the *Helvetoglobotruncana helvetica* Zone, from the top of the lower Turonian. Moreover, the ammonites collected in this study, along with the results of Meister and Rhalmi (2002), Kennedy et al. (2008), Cavin et al. (2010), Lezin et al. (2012) and Meister and Piuz (2013), allow us to recognize (1) the Guerangeri Zone, lower upper Cenomanian, in the lower part of the Akrabou Formation and (2) the Nodosoides Zone, upper lower Turonian, in the upper part of the same Formation.

The OAE2 is marked worldwide by a positive $\delta^{13}C$ excursion (Tsikos et al., 2004; Sageman et al., 2006; Grosheny et al., 2008; Elrick et al., 2009; Jati et al., 2010), also recorded in the Preafrican Trough (Lezin et al., 2012; Lebedel et al., 2013) at the top of the *R. cushmani* Zone and at the extreme base of the *W. archaeocretacea* Zone, and ranging up to the Cenomanian/Turonian boundary (Figs. 3 and 4). Worldwide, this excursion is dated as late Cenomanian (Gale et al., 1993, 2005; Kuhnt et al., 2004; Tsikos et al., 2004; Caron et al., 2006; Westermann et al., 2010; Bomou et al., 2013) and corresponds to the time interval during which dysoxic/anoxic conditions were most extensively developed. We chose to call this period the CCIE (Cenomanian Carbon Isotope Excursion), in order to differentiate it from the OAE2 that lasts longer. Indeed, many studies (Terrab, 1994; El Albani et al., 1997; Friedrich et al., 2006; Grosheny et al., 2008; Van Bentum et al., 2009; Jati et al., 2010; Monteiro et al., 2012) show that dysoxic/anoxic conditions related to the OAE2 are locally present before and/or after this CCIE.

The stratigraphic studies of Ettachfini and Andreu (2004) and Ettachfini (2006) show that the Cenomanian/Turonian boundary is a major regional discontinuity (D4) over a large part of the Morocco Basins (Preafrican Trough, High Moulouya, Middle Atlas and High Atlas synclines). In the Preafrican Trough, D4 picks out an important change in the sedimentation, with the appearance of thinly-bedded limestone, often laminated and rich in cherts. These authors (*op. cit.*) also noted a great abundance of Heterohelicidae at around the Cenomanian/Turonian boundary, corresponding to the "*Heterohelix shift*", which is also recognized in Tunisia (Robaszynski et al., 1990; Nederbragt and Fiorentino, 1999; Caron et al., 1999; Abdallah, 2000) and in the central High

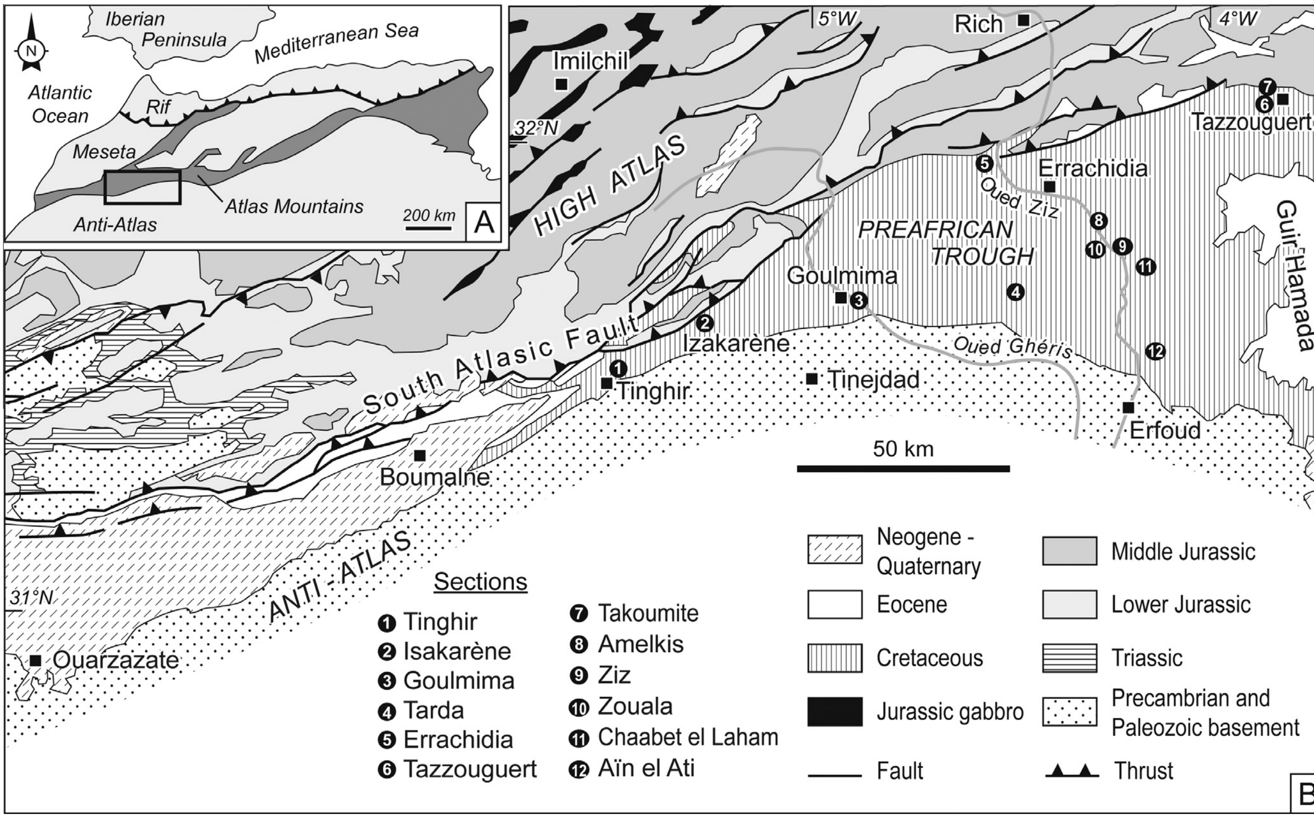

Fig. 1. (A) Map of North Africa and location of the Preafrican Trough, Morocco; (B) geological map of the High Atlas and the Preafrican Trough, and location of the twelve studied sections.

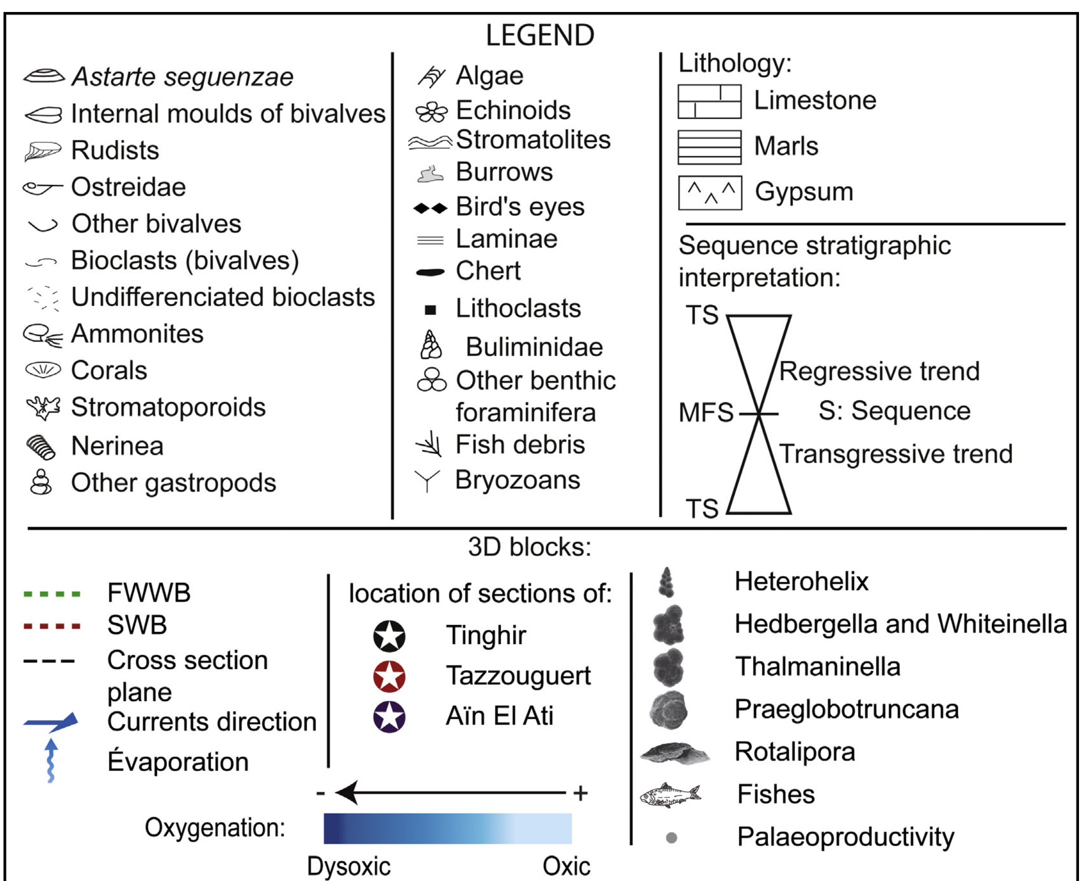

Fig. 2. Legend for Figs. 3–9. TS: transgressive surface; MFS: maximum flooding surface; FWWB: fair-weather wave base; SWB: storm wave base.

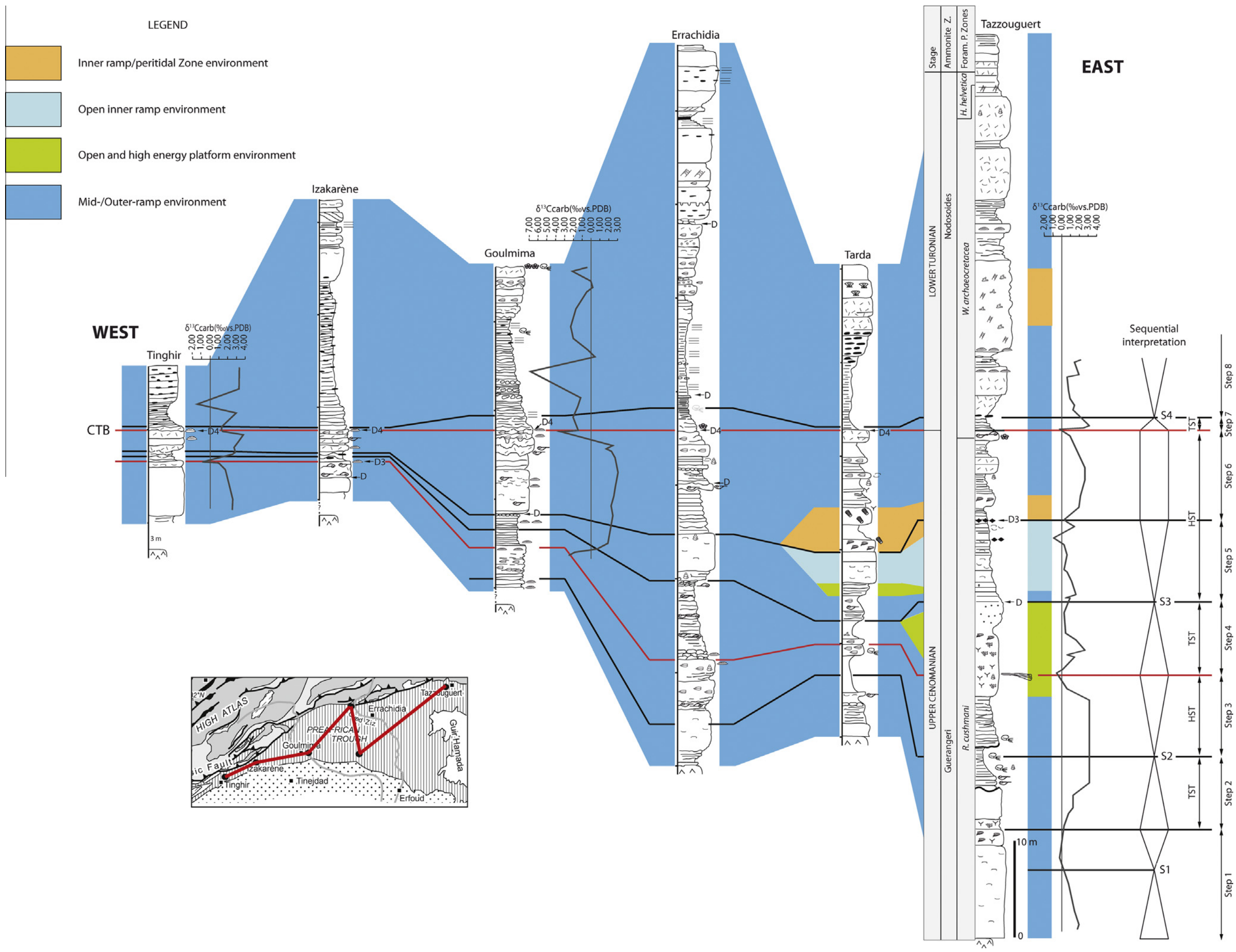

Fig. 3. Stratigraphic correlations and evolution of depositional environments on the Preafrican Trough carbonate platform, along a west-east transect (indicated by the red line on the map) between the Tinghir and Tazzouguert sections. The $\delta^{13}C$ values of the Tinghir, Goulmima and Tazzouguert sections are also shown. Four third-order sequences, named S1–S4, can be defined. The red lines indicate the limits of the CCIE. D: discontinuity (D3 and D4 are major regional discontinuities). HST: Highstand System Tract. TST: Transgressive system Tract. See legend in Fig. 2. (For interpretation of the references to colour in this figure legend, the reader is referred to the web version of this article.)

Atlas, Morocco (Ettachfini et al., 2005). Finally, D4 occurs just at the end of the $\delta^{13}C$ positive excursion in the Preafrican Trough sections, the Mibladen section in the High Moulouya, and the Ben Cherrou section in the central High Atlas (Ettachfini and Andreu, 2004; Ettachfini, 2006; Lezin et al., 2012; Lebedel et al., 2013). In this last section, the presence of *Watinoceras* sp. (ammonite) just above D4 provides an additional argument that this discontinuity represents the Cenomanian/Turonian boundary (Ettachfini, 2006).

2.3. Facies, environments and stratigraphy

The sedimentological, lithological and palaeontological analysis of twelve sections of the upper Cenomanian–lower Turonian of the Preafrican Trough allowed to define seventeen facies, named F1–F15, first described in Lezin et al. (2012) and further detailed in this study (Table 1). Each facies is characterized by typical skeletal and non-skeletal components (macro and micro), as well as specific textural features and sedimentary structures. These facies can be attributed to seven depositional environments, ranging from the peritidal zone and restricted lagoon to the deep open platform (Table 1). The interpretation of the palaeoenvironments is discussed in detail in Lezin et al. (2012) and Lebedel (2013).

The facies is determined for each sample in all the studied sections (a total of 659 samples). A middle to outer ramp facies (F1–F4) predominates in the Goulmima section (Lezin et al., 2012), as also observed in the other western sections (Tinghir, Izakarène, Errachidia and Tarda). By contrast, the Tazzouguert (Lebedel et al., 2013) and the other eastern sections (Takoumite, Amelkis, Ziz, Zouala, Chaabet El Ham and Aïn El Ati) are characterized by depositional environments ranging from the peritidal zone to the deep outer ramp (facies F1–F15). The deep outer ramp environment (facies F1–F4) appears mainly during the Turonian.

Thus, during most of the late Cenomanian (just before and during the CCIE), the platform displays an East–West polarity, with an opening toward the west. Shallow environments of the inner ramp/peritidal zone dominate in the eastern part of the platform, associated with an abundant and diverse fauna, while deeper environments of the mid/outer ramp are more prevalent in the western part, with rare and poorly diversified fauna, mainly composed of bivalves and opportunist benthic and planktonic foraminifera. The base of the lower Turonian is marked by flooding of the platform: an outer ramp environment is established over the entire platform, which becomes colonized by abundant opportunistic benthic and surface planktonic foraminifera (*Whiteinella*, *Heterohelix* and *Hedbergella*).

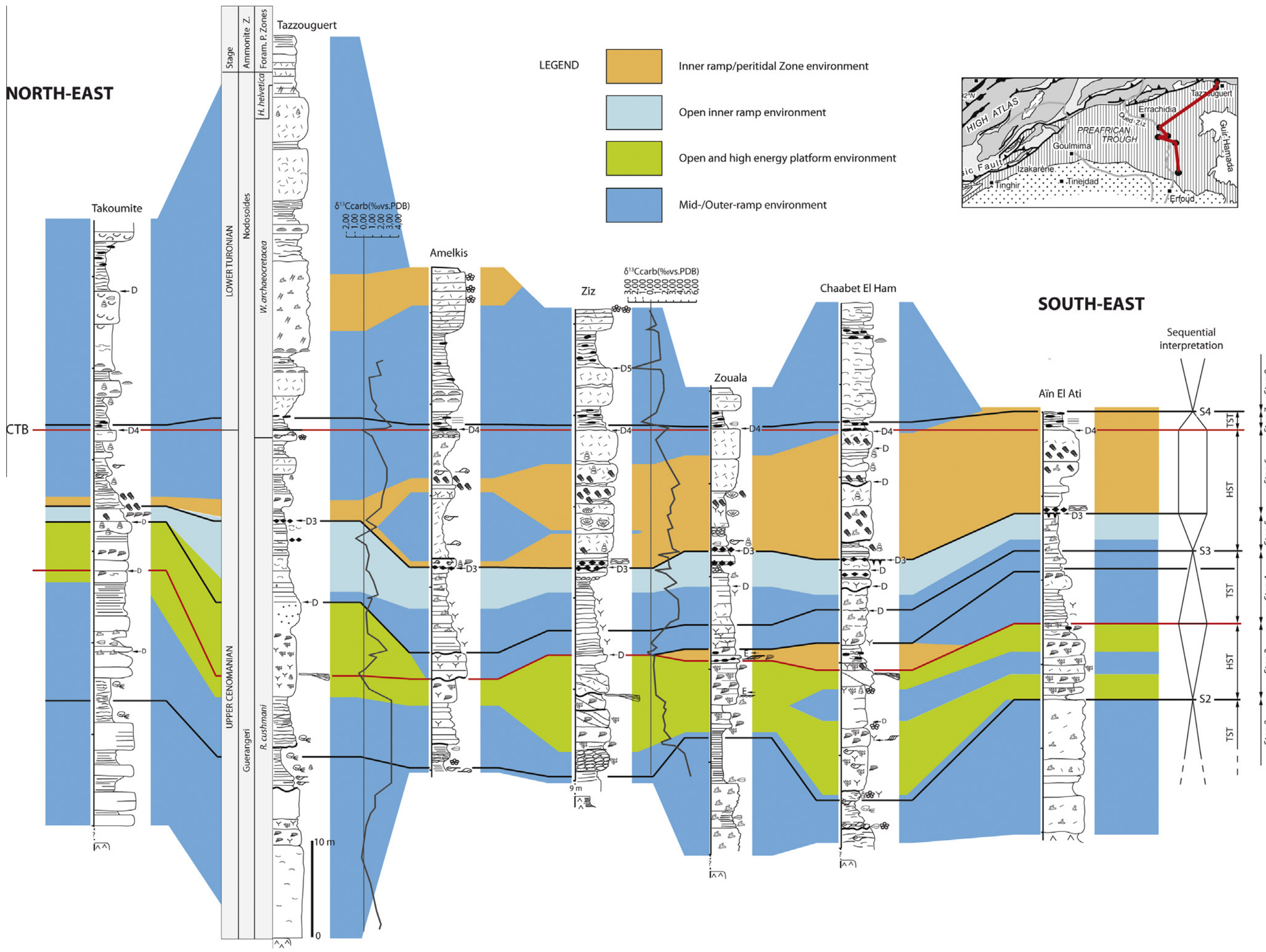

Fig. 4. Stratigraphic correlations and evolution of depositional environments on the eastern part of the Preafrican Trough carbonate platform, along a north–south transect (indicated by the red line on the map) between the Takoumite and Aïn El Ati sections. The $\delta^{13}C$ values of the Tazzouguert and Ziz sections are also shown. Four third-order sequences, named S1–S4 were determined. The red lines indicate the limits of the CCIE; D: discontinuity (D3 and D4 are major regional discontinuities). HST: Highstand System Tract. TST: Transgressive system Tract. See legend in Fig. 2. (For interpretation of the references to colour in this figure legend, the reader is referred to the web version of this article.)

A study of the distribution of palaeoenvironments over time allows us to characterize their spatial and temporal variations, leading to the identification of sequence stratigraphy. Indeed, by using correlations based on the biostratigraphic and geochemical ($\delta^{13}C$) data, as well as the sequence-stratigraphy interpretation of the different sections, we are able to divide the sedimentary succession of the upper Cenomanian–lower Turonian of the Preafrican Trough into four 3rd-order sequences, denoted S1–S4 (Lezin et al., 2012; this study). However, a few changes have been made compared to Lezin et al. (2012) especially the paleogeographic interpretation during the S1 sequence and the chronostratigraphic position of the S4 sequence boundary. The S4 sequence boundary was originally positioned at an emersion discontinuity dated from the late Cenomanian (Lezin et al., 2012). The study of three additional sections shows that, above this emersion surface, in the eastern part of the Preafrican trough, the accommodation space increases whereas, in the western part, the accommodation space decreases. These different trends are only due to differential subsidence. That is the reason why the upper part of the upper Cenomanian is integrated in the regressive trend of the sequence S3. In this new interpretation, the S4 sequence boundary is positioned at the D4 discontinuity. An important increase in the accommodation space (transgressive trend) is recorded above this last discontinuity. So, in the present study, we propose new stratigraphic correlations based on two transects: (1) an east–west transect, from Tinghir to Tazzouguert, running across the sections of Izakarène, Goulmima, Errachidia and Tarda (Fig. 3), and (2) a north–south transect, in the eastern part of the platform, extending between the sections of Takoumite and Aïn El Ati, via the sections of Tazzouguert, Amelkis, Ziz, Zouala and Chaabet El Ham (Fig. 4).

2.4. Oxygenation and palaeoproductivity conditions

Lebedel et al. (2013) compared geochemical (major, minor and trace elements), palaeontological and sedimentological data to determine the oxygenation and palaeoproductivity conditions on the platform. During the early Cenomanian and the CCIE, slightly dysoxic conditions were present in the bottom waters of deeper environment (mid to outer ramp) over the western part of the platform, while the eastern waters were oxic. The palaeoproductivity was low over the entire platform. The dysoxia of bottom waters recorded in the west is related to the influx of poorly-oxygenated waters from the deeper anoxic basins of the Atlantic and/or Tethys Oceans, which occurred during the Cenomanian second-order transgression (Hardenbol et al., 1998). In contrast, during the early Turonian, highly dysoxic bottom and intermediate waters were present over the entire platform. This Turonian dysoxia was

Table 1
Characteristics and interpretations of facies defined in the Preafrican Trough platform deposits (modified after Lezin et al., 2012). FWWB: fair-weather wave base; SWB: storm wave base.

Facies numero	Lithofacies	Main skeletal and non skeletal components	Sedimentary structures	Depositional interpretation
F15a	Fenestral micrite	Rare miliolids (*Istriloculina* sp.) – rare pellets and root traces – planktonic foraminifera – some small textulariids, *Valvulineria* sp. and ostracods	Abundant fenestrae or birdseye fabrics	Peritidal Zone
F15b	Stromatolitic boundstone	Stromatolites and peloids	Birdseye fabrics	
F14–15	Benthic foraminifera-bearing wackestone/packstone	Abundant benthic foraminifera (dominance of miliolids, *Pseudorhapydionina* sp. and little textulariids) – echinoids – planktonic foraminifera – gasteropods – lithoclasts	Rare birdseye fabrics	Inner Ramp (above FWWB) with restricted conditions (lagoon)
F14	Miliolid-bearing mudstone/wackestone	Few miliolids (dominance of *Istriloculina* sp.) – rares bioclasts, *Bacinella irregularis* and allochtonous foraminifera		
F13	Nerinea wackestone to grainstone	Abundant *Nerinea* – echinoids – red algae – ostracods – rare benthic foraminifera (Nezzazatids, lituolids, textulariids, *Cuneolina* sp., *Pseudolituonella reicheli*...)		Inner Ramp (above FWWB) with normal conditions (lagoon)
F12	Dasycladacean algae-coral wackestone	Numerous dascycladales – scleratinian corals – rares ostracods, gastropods, benthic foraminifera (miliolids, nezzazatids, *Cuneolina* sp., *Charentia* sp...)		
F11	Large benthic foraminifera wackestone/packstone	Numerous and diversified large benthic foraminifera (alveolinids, large miliolids, *P. reicheli*, *Dicyclina* sp., *Spirocyclina atlasica*, *Chrysalidina gradata*, nezzazatids, textulariids)		
F10	Biodetrital grainstones	Lithoclasts – allochtonous bioclasts (corals, rudists, red and green algae, echinoids, gastropods) – rare benthic foraminifera	Sigmoidal clinoforms	Inner ramp (above FWWB): high-energy open platform
F9	Nezzazatid-bearing peloidal packstone/grainstone	Abundant *Nezzazata simplex* – textulariids – abundant fragments of echinoids – some bivalve shells	Sandbars with sigmoidal structures	
F8	Floatstone/packstone with biodetrital rudists	Abundant rudists (radiolitids, intact and fragmented) and intraclasts – ostracods – echinoids – benthic foraminifera (textulariids, nezzazatids, rares lituolids, *P. reicheli*, *Cyclorbiculina iranica* and miliolids)		
F7	Floatstone/wackestone with rudists and stromatoporoids	Abundant rudists (requienids and radiolitids) – stromatoporoids – echinoids – abundant and diversified benthic foraminifera (nezzazatids, textulariids, miliolids, *Pseudolituonella* sp. . .)		Mid-ramp (between FWWB and SWB)
F6	Stromatoporoids boundstone	Abundant stromatoporoids – Presence of bryozoans, solitary corals, bivalves, echinoids, gastropods, *Permocalculus* sp. and benthic foraminifera (miliolids, nezzazatids, textulariids, *P. reicheli* and *Gaudryina* sp.)		
F5	Bryozoan-bearing floatstone/wackestone	Abundant bryozoans – rare bivalves, echinoids fragments, serpulids, miliolids, textulariids and *P. reicheli*		
F4	Bivalve-bearing biodetrital packstone/grainstone	Abundant reworked bivalve shells – presence of gastropods and lithoclasts – rare echinoids, benthic and planktonic foraminifera – organisms filled with peloïds and crustacean coprolites		
F3	Bivalve-bearing floatstone	Abundant bivalves (including abundant oysters) – very rare benthic foraminifera	Thinly-bedded marls	
F2–3	Bivalve-bearing wackestone	Abundant fragments of oysters – presence of fragments of echinoids, gastropods and *Permocalculus* sp. – rare ostracods, benthic and planktonic foraminifera		Outer ramp (below SWB) – normal oxygenation conditions
F2	Foraminiferal mudstone	Abundant planktonic foraminifera – rare benthic foraminifera and oyster		
F1	Mudstone with or without buliminids	Assemblage of small opportunistic benthic foraminifera (e.g. buliminids), fish vertebrae and phosphatic bioclasts – rares calcispheres and/or planktonic foraminifera – Abundant cherts	Thinly-bedded micritic limestones, often laminated	Outer ramp (below SWB) – dysoxic conditions

due to an increase of the palaeoproductivity, which enhanced the consumption of O_2 owing the decay of organic matter. These results are supported by the studies of Andreu et al. (2013) on the ostracods of the Preafrican Trough.

2.5. Clay mineralogy and climate

A clay mineral study was performed on three sections: Tinghir (17 samples), Izakarène (30 samples) and Goulmima (23 samples). The analyses were carried out at the Geoscience Environnement Toulouse (France) laboratory, using X-ray diffraction (with a G3000 INEL instrument) on decarbonated samples. The intensities of the identified minerals are measured for a semi-quantitative estimate of clay minerals, expressed in relative percent without correction factors, because of the small error margin (<5%). Finally, we have distinguished three time periods (before, during and after the CCIE). For each, on the three sections studied, the average content of the different clay minerals is calculated.

Clay mineral data are not available for the base of the upper Cenomanian, before the CCIE). However, the presence of evaporites (gypsum) in the western part of the Preafrican Trough (Lebedel, 2013) suggests a dry climate.

Clay assemblages in the three sections consist of kaolinite, palygorskite, illite, smectites and illite–smectites (I/S) mixed layers (Fig. 5). The upper Cenomanian sediments, deposited just before and during the CCIE, are marked by the presence of palygorskite (up to 42%), illite (12–33%) and smectites (up to 36%), associated with minor amounts of I/S mixed layers (5–29%). Kaolinite is present only occasionally at Tinghir and Goulmima, with a maximum abundance of 38%. After the CCIE, palygorskite disappears during the early Turonian, along with smectites that are present only episodically at Goulmima (12% average), in favour of illite (up to 85% in Goulmima) and kaolinite (Tinghir and Izakarène, up to 72%).

The shallow burial depth of the Cretaceous deposits of the Preafrican Trough and the SEM observations of the clay minerals (Lebedel, 2013) indicate that they have a mainly detrital origin. Therefore, these minerals can be used as a climatic proxy. Kaolinite of detrital origin is formed under humid conditions in equatorial well drained soils (Deconinck et al., 1982). Smectites appear in tropical soils under a warm climate with contrasted seasons. The palygorskite forms in environments rich in cations (Chamley, 1989) such as lagoons, in the immediate surrounding areas of continents and lakes, as well as in desert soils (Thiry and Pletsch, 2011). Illite is a primary mineral produced by the

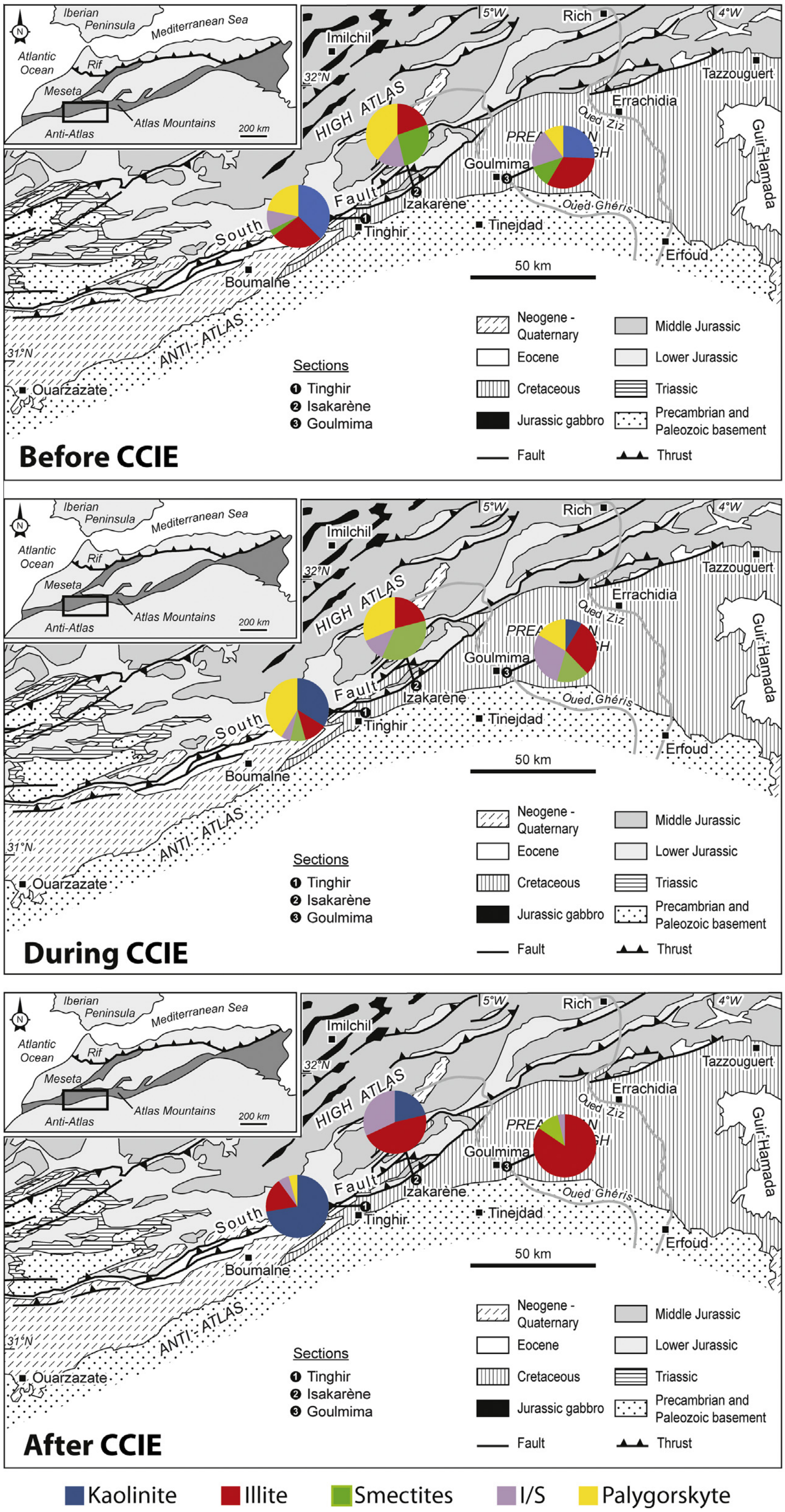

Before CCIE	Tinghir	Izakarène	Goulmima
Kaolinite	38	0	26
Illite	27	20	33
Smectites	3	27	11
I/S	10	14	20
Palygorskite	22	39	10

During CCIE	Tinghir	Izakarène	Goulmima
Kaolinite	34	0	9
Illite	12	21	29
Smectites	8	36	17
I/S	5	12	29
Palygorskite	42	31	16

After CCIE	Tinghir	Izakarène	Goulmima
Kaolinite	72	21	0
Illite	18	47	85
Smectites	0	0	12
I/S	6	32	4
Palygorskite	4	0	0

Fig. 5. Evolution of clay mineral abundances in time and space on the Preafrican Trough platform. Each value (given in%) represents the average relative abundance of the different clay mineral species in the three studied sections (Tinghir, Izakarène and Goulmima).

mechanical weathering of pre-existing rocks in a hot and dry climate, or in very cold climates at high latitude, or alternatively in areas of high relief or tectonically active zones.

So, during the late Cenomanian (just before and during the CCIE), the detrital flux derived from the Preafrican Trough was both primary (illite) and pedogenic (smectites and kaolinite) in origin. This detrital supply probably came from the erosion of the Anti-Atlas, to the south of the platform, in an area affected by pedogenic processes under warm climatic conditions with contrasted seasons (presence of smectites). The presence of allochthonous

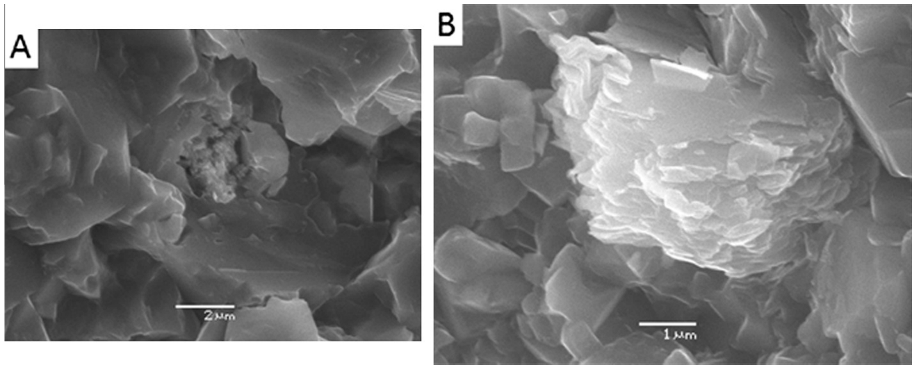

Fig. 6. SEM observations: (A) palygorskite (upper Cenomanian–Tinghir section) forming a mass (centre of photo) that fills the intercrystalline porosity. Their poor crystallinity rules out a diagenetic origin and supports a detrital origin. (B) Kaolinite (lower Turonian–Tinghir section).

palygorskite (Fig. 6A) can be explained by an input coming from the surrounding evaporite basins, or the reworking of ancient evaporitic deposits of the Aoufous Formation. During the early Turonian, the predominance of detrital kaolinite (Fig. 6B) and the disappearance of smectites (except at Goulmima) and palygorskite could be explained by the establishment of a hot and wet climate. Nevertheless, this scenario remains only a hypothesis, because the very low abundance of clay (<1%) in the Turonian limestones of the Preafrican Trough sections can disturb this climate reconstruction.

3. Platform configuration and palaeoenvironmental conditions

The palaeoenvironmental and relative sea level variations of the Preafrican Trough carbonate platform during the late Cenomanian–early Turonian can be summarized in eight steps (Figs. 7–9), using all the previously described data.

3.1. Late Cenomanian, before the CCIE, R. cushmani Zone

In the eastern part of the platform, open marine sedimentation begins with the establishment of a mid/outer-ramp environment above the gypsiferous marls of the Aoufous Formation (Sequence S1 on Fig. 3 and step 1 on Fig. 10). This marine environment is characterized by the appearance of yellowish mudstone, more or less rich in planktonic foraminifera and oysters. In the west, gypsiferous marls typical of lagoonal or paralic sebkrah environments (Ettachfini, 2006) are still present. The climate is dry, the waters are well-oxygenated and the palaeoproductivity is low.

Then, during accumulation of the Guerangeri Zone, an outer ramp environment appears in the eastern part of the platform, with the development of yellow nodular marls, more or less rich in ammonites (*Neolobites vibrayeanus*), planktonic foraminifera and echinids (base of S2 in Fig. 3; step 2 on Fig. 10). These open marine conditions gradually extend towards the western part of the Preafrican Trough (Fig. 7A). As observed farther west, the climate is dry, with well-oxygenated waters and low palaeoproductivity.

Just before the CCIE, at the top of the Guerangeri Zone, the polarity of the platform changes (Fig. 7B), becoming open and deeper toward the west (top of S2 on Fig. 3; step 3 on Fig. 10). This polarity remains unchanged up until the early Turonian. The determining factor explaining this sudden change is very likely tectonic. We hypothesize that this sudden change is linked to the activation of a generally N-S trending fault (in the Antiatlasic basement?), which accounts for the present-day course of the Ziz wadi (Fig. 1). In the eastern part of the platform, bioclastic sandbars prograde to the south (top of S2 on Fig. 4), associated with, abundant stromatoporoids and rudists between the bars. These facies characterize an open high-energy environment. In the west, bioclastic limestones with ostreids, *Astarte saguenzae* and internal moulds of bivalves are deposited in a mid to outer ramp environment; buliminids are present in the western part. The climate is warm with contrasted seasons, while the marine environment shows low palaeoproductivity. In the east, the waters are well-oxygenated while, in the west, bottom the waters are dysoxic.

3.2. Late Cenomanian, during the CCIE: top of the R. cushmani Zone-extreme base of the W. archaeocretacea Zone

At the base of the CCIE, in the south-eastern part of the Preafrican Trough (Amelkis, Zouala, Chaabet El Ham and Aïn El Ati sections), an open mid-ramp environment is characterized by a predominance of bryozoans associated with numerous burrows (base of S3 on Figs. 4 and 8A; step 4 on Fig. 10). This environment passes laterally, toward the north-east (Tazzouguert and Takoumite sections), into a shallower high-energy open platform, characterized by facies with rudists and stromatoporoids. Towards the west, a calm and deep marine environment (outer-ramp) is indicated by the development of interbedded marls and limestones containing rare ostreidae, planktonic foraminifera, calcispheres and buliminids, sometimes associated with silicification. Thus, during this interval of time, the platform is open toward the south and the west, where the environments are deeper. The climate is warm with contrasted seasons, while the marine environment shows low palaeoproductivity associated with well-oxygenated waters, except for dysoxic bottom waters in the west.

Then, a rapid fall in relative sea-level leads to the establishment of sub-emergent conditions in the east (birdseye fabrics, stromatolites, and sometimes desiccation cracks; middle of S3 on Figs. 4 and 8B; step 5 on Fig. 10). In the west, the mid to outer-ramp environment persists, mainly leading to the accumulation of bioclasts of bivalves reworked by storms. The regional D3 discontinuity formed at the end of this episode represents the lowest relative sea level of the late Cenomanian–early Turonian, in the Preafrican Trough. The climatic conditions, as well as the oxygenation and palaeoproductivity levels, are similar to those of the previous episode (step 4).

At the end of the CCIE, in the eastern part of the platform, the sub-emergent facies is rapidly covered by aggrading facies typical of the peritidal zone (birdseye fabrics, stromatolites) and inner ramp (*Nerinea*, alveolinids and miliolids) (top of S3 on Figs. 4; 9A; step 6 on Fig. 10). This shallow environment is crossed by tidal channels. Then, a progressive opening of the platform from the north is recorded, with deeper water environments (bivalves, phosphate and occasionally planktonic foraminifera) established first in the north-east (Takoumite), which gradually move

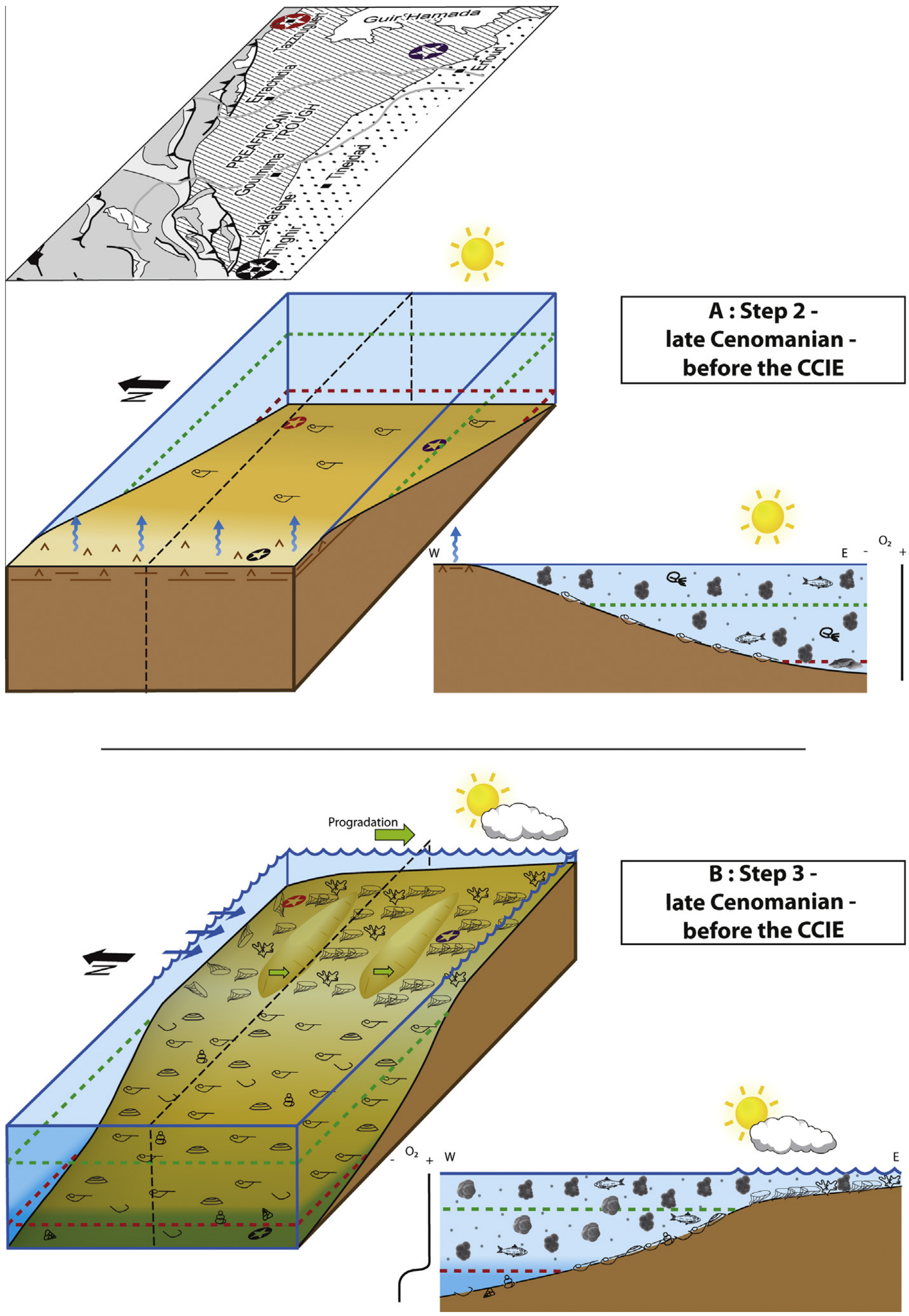

Fig. 7. Schematic diagrams of the Preafrican Trough platform, in 3D and in cross-section, in the late Cenomanian (before the CCIE), during: (A) the transgressive episode of sequence S2, (B) the regressive episode of sequence S2. See legend in Fig. 2.

southwards to reach Zouala and Chaabet El Ham at the end of the step (Fig. 4). This succession reflects the deposition of an aggrading sequence following an increase of accommodation space. In the western part of the platform, thin beds of shelly limestone are developed, bounded by erosive surfaces. These facies reflect storm-influenced sedimentation, and their vertical succession suggests stability, and even a slight reduction of accommodation space. In this way, differential subsidence is recorded across the platform: in the eastern part, the ratio of accommodation space to carbonate production is slightly greater than 1, whereas the same ratio is slightly less than 1 in the western part. Subsidence is more marked (1) in the east than in the west of the platform and (2) in the north-eastern than in the south-east. Sedimentation takes place during a phase of high sea level, coinciding with a global creation of accommodation space that ceases at the D4 discontinuity. The climate is warm with contrasted seasons, while the waters are well-oxygenated, except in the west where the bottom waters are dysoxic and the palaeoproductivity is low.

3.3. Early Turonian, after the CCIE: top of the W. archaeocretacea Zone–base of the H. helvetica Zone

An abrupt change in the sedimentation is recorded just above D4 (step 7 on Fig. 10). The flooding of the platform (drowning phase; base of S4 on Figs. 3, 4 and 9B) is reflected by the presence of "lag" facies just above this discontinuity on the western sections, as well as the appearance of thinly-bedded grey micritic limestone,

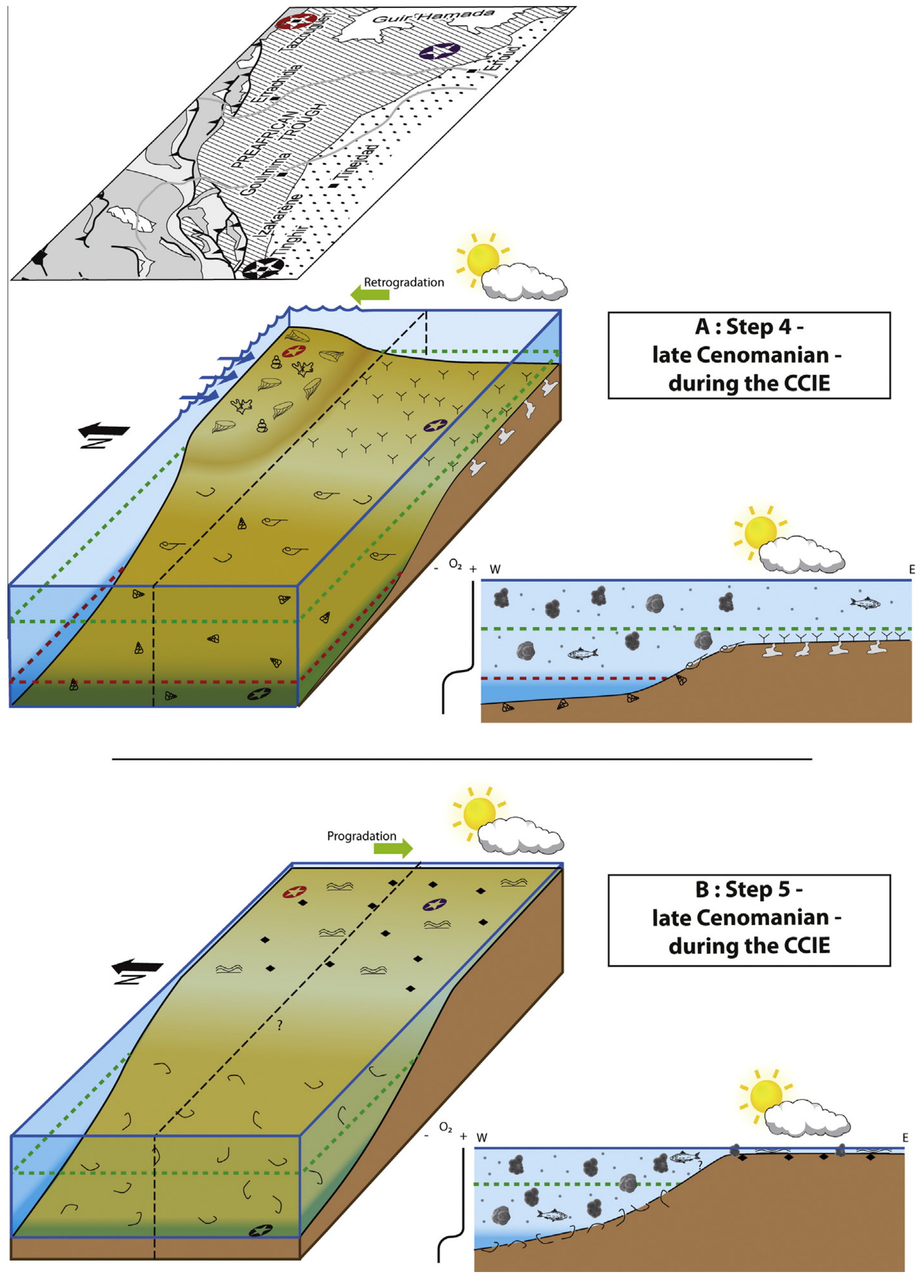

Fig. 8. Schematic diagrams of the Preafrican Trough platform, in 3D and in cross-section, in the late Cenomanian (during the CCIE), during: (A) the transgressive episode of sequence S3, (B) the onset of the regressive episode of sequence S3, around the D3 discontinuity. See legend in Fig. 2.

often laminated, that are rich in phosphates and yellow chert nodules. An outer ramp environment appears on the platform, where flora is absent and the fauna is dominated by small opportunistic benthic forams (buliminids; Koutsoukos et al., 1990; Ly and Kuhnt, 1994; Friedrich et al., 2006; Friedrich, 2010) and planktonic forams (*Guembelitria cretacea*, *Heterohelix globulosa*, *Whiteinella* sp.) associated with fish debris. This interval records the highest relative sea level of the platform during the late Cenomanian–early Turonian. The bottom and intermediate waters are very dysoxic over the entire platform, linked to a major increase in palaeoproductivity induced by enhanced nutrient supply (Andreu et al., 2013; Lebedel, 2013; Lebedel et al., 2013). The climate is probably hot and wet.

In the last episode (step 8 on Fig. 10), mid-ramp type sedimentation gradually reappears in a context of high sea-level, with the return of bioclastic limestones containing gastropods, bivalves, benthic and planktonic foraminifera (top of S4 on Fig. 4). The waters are poorly-oxygenated at the onset of step 8, and oxic at the end. Palaeoproductivity falls to low levels at the end of this step. The platform probably disappears at the end of the early Turonian.

4. Discussion

4.1. Trophic conditions

Nutrient availability is one of the main factors controlling the development of a platform. In the Preafrican Trough, during the upper Cenomanian, before and during the CCIE, the presence of numerous and diversified carbonate producers (rudists, bryozoans, large benthic foraminifera, planktonic foraminifera, etc.) indicates

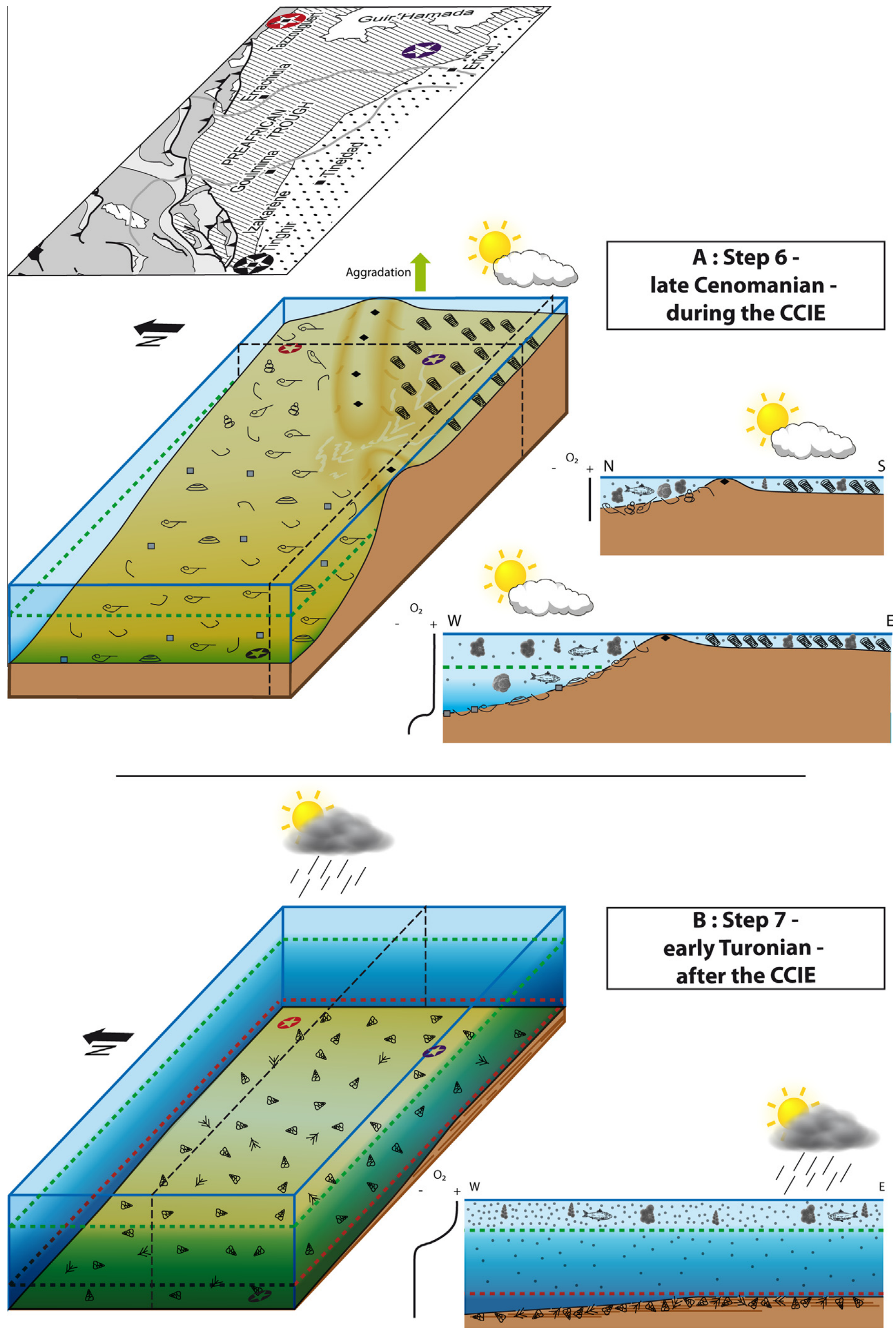

Fig. 9. Schematic diagrams of the Preafrican Trough platform, in 3D and in cross-section, in (A) the late Cenomanian (during the CCIE), at the end of the regressive episode of sequence S3, (B) the early Turonian (after the CCIE), during the transgressive episode of sequence S4. See legend in Fig. 2.

oligotrophic to mesotrophic conditions (Föllmi et al., 1994; Voigt et al., 1999; Parente et al., 2008; Gebhardt et al., 2010). The geochemical proxies of palaeoproductivity (Cd, Ni, P and Zn) used by Lebedel et al. (2013) show little enrichment, which argues for a low-medium levels of palaeoproductivity. Thus, the low regional palaeoproductivity levels recorded in the Preafrican Trough during the late Cenomanian, and more specifically during the CCIE, show a trend running counter to the global record, which indicates high palaeoproductivity conditions contributing to the establishment of global anoxia (Mort et al., 2007; Jenkyns, 2010; Monteiro et al., 2012).

During the lower Turonian, the high concentrations of Cd, Ni P, Si and Zn are indicative of high organic productivity (Lebedel et al., 2013), which is recorded throughout the Preafrican Trough. Eutrophic conditions are indicated by the enrichment of these trace metals, associated with the disappearance of the majority of the Cenomanian biota, along with the predominant occurrence of buliminids and opportunistic planktonic foraminifera (“*Heterohelix shift*” in Goulmima), as well as the significant increase of fish debris (Friedrich et al., 2006; Gebhardt et al., 2010). The establishment of these eutrophic conditions could be due to enhanced nutrient inputs, caused by a mechanism such as intense continental weathering (Jenkyns, 2010; Monteiro et al., 2012) and/or upwelling systems (Trabucho Alexandre et al., 2010). This increase in palaeoproductivity could have contributed to the drowning of the platform, by disrupting the development of

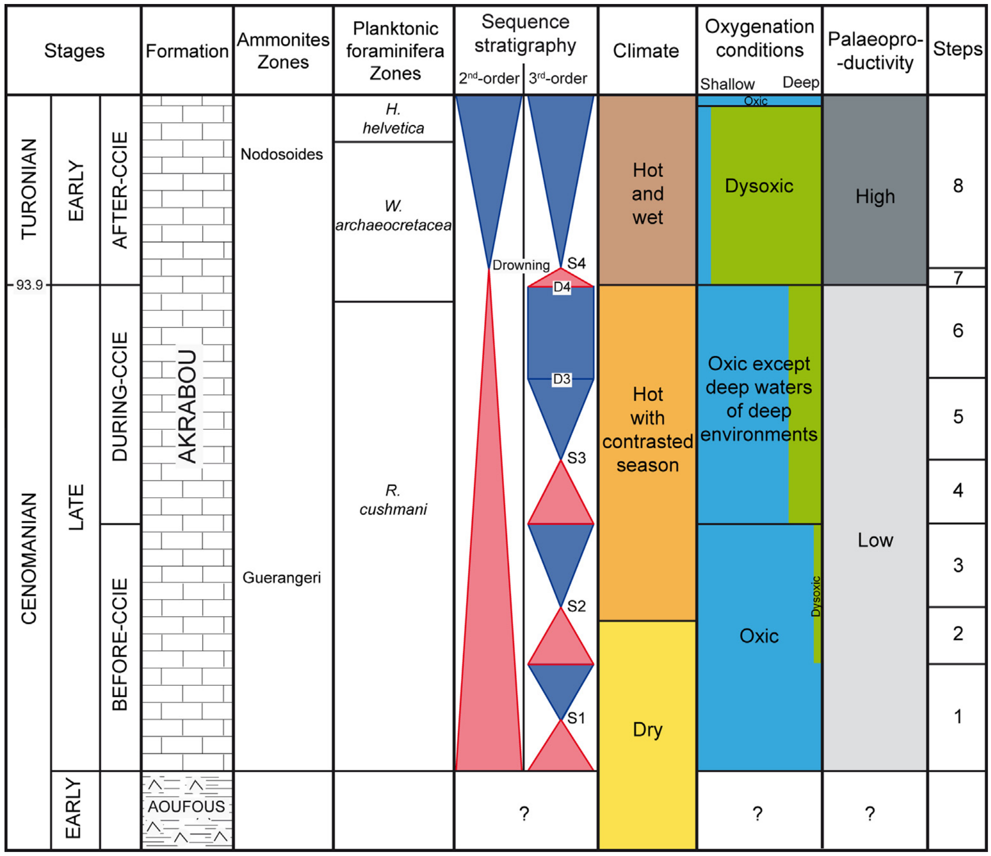

Fig. 10. Diagram summarizing the stratigraphic framework and different conditions (transgression–regression phases, climate, oxygenation and palaeoproductivity conditions) existing in the Preafrican Trough during the late Cenomanian–early Turonian. The time-range of each step (see part 3) is also represented. D3 and D4: major regional discontinuities.

carbonate producers (Föllmi et al., 1994; Drzewiecki and Simo, 1997; Voigt et al., 1999).

4.2. Climatic record

Before the CCIE, the Preafrican Trough shows a low palaeoproductivity under an arid climate. It remains low during the CCIE, but under a warm climate with contrasted seasons. This climate evolution is in agreement with the data from several authors (Jenkyns et al., 2004; Steuber et al., 2005; Friedrich et al., 2011; Monteiro et al., 2012) who consider that the global climate was warmer and wetter during the CCIE than before. According to these authors (op cit.), this climate change would produce an increase of chemical weathering on the continents, leading to a higher input of dissolved inorganic matter into the oceanic basins. These solutes serve as nutrients to the organisms, favouring the onset of intense productivity and allowing the establishment of global dysoxia/anoxia (Monteiro et al., 2012). This hypothesis, which is one of the main hypothesis explaining the establishment of a global dysoxia during the CCIE, is not supported over a large part of the Saharan platform, because of the development of (1) photozoan carbonate-producing ecosystems composed of rudists, stromatoporoids, green algae, benthic foraminifera and rare corals, which are widespread in tropical and subtropical environments, then (2) heterozoan carbonate producers, composed of bryozoan, benthic foraminifera and bivalves. The development of numerous oligotrophic platforms, as observed in Egypt, the Czech Republic, Iraq, Morocco, Oman, Algeria, Tunisia, Mexico, etc. (Philip et al., 1995; Aguilera-Franco and Romano, 2004; Grosheny et al., 2008, 2013; El-Shazly et al., 2011; Lezin et al., 2012; Al-Dulaimi et al., 2013) in an interval of time characterized by an anoxia/dysoxia at the global scale, does not argue in favor of a continental origin for intense productivity during the CCIE.

During the early Turonian, a hot and wet climate seems to appear on the Preafrican Trough (Fig. 10). The development of this climate is consistent with the studies of Voigt et al. (2004), Sinninghe Damsté et al. (2008), Jarvis et al. (2011) and Van Bentum et al. (2012) who evoke a climatic optimum recorded at the base of the lower Turonian, after the CCIE.

4.3. Variation of relative sea level and drowning of the platform

In the western part of the Saharan platform, drowning of the platform is recorded in different areas. In the Preafrican Trough, the appearance of thinly-bedded limestone just above the D4 discontinuity marks a 2nd-order eustatic maximum. In the Agadir basin, the appearance of black shales in the lower Turonian is coeval with a major transgression (Jati et al., 2010). In the High Atlas synclines and the High Moulouya, Ettachfini (2006) notes a transgressive trend just above the Cenomanian/Turonian boundary which is marked by the appearance of thinly-bedded micritic limestone rich in planktonic foraminifera. In the Guir Basin (southwest Algeria), Benyoucef and Meister (2015) observe a flooding of the early Turonian platform, marked by the establishment of thin lime-mudstone beds. Moreover, around the C/T boundary, many other platforms undergo a phase of sudden drowning, for example in Italy (South Apeninnes; Parente et al., 2007), Mexico (Hernàndez-Romano et al., 1997), Spain (Drzewiecki and Simo, 1997), Germany (Wilmsen et al., 2010), Yugoslavia (Jenkyns, 1991), Oman (Philip et al., 1995) and Jordan (Schulze, 2003).

These drowning phases seems mainly related to (1) the high sea level stand after the major transgression of the late Cenomanian

(Philip and Airaud-Crumiere, 1991; Hernàndez-Romano et al., 1997; Parente et al., 2007) and (2) the presence of a high palaeoproductivity, unfavorable for the development of carbonate producers (Hernàndez-Romano et al., 1997) and causing the formation of poorly-oxygenated waters. Indeed, some authors also note the presence of dysoxic/anoxic conditions during the late Cenomanian–early Turonian in platform environments (Philip and Airaud-Crumiere, 1991) in Morocco (Lebedel et al., 2013), Egypt (Gertsch et al., 2010b; El Sabbagh et al., 2011), Mexico (Hernàndez-Romano et al., 1997) and Jordan (Schulze et al., 2005). On these platforms, the dysoxic/anoxic conditions are recorded during phases of relative sea level rise, and even sometimes during drowning of the platforms. In the very shallow environments, the waters remain well-oxygenated because of the exchanges with the atmosphere.

4.4. OAE2 dysoxia/anoxia on the western part of the Saharan platform

The review study of Monteiro et al. (2012) shows that dysoxic/anoxic conditions existed before the CCIE (upper Cenomanian) in tropical Central Atlantic: Tarfaya basin (Morocco), Demerara rise (Suriname), Maracaibo Basin (Venezuela) and Cap Verde. This pre-CCIE dysoxia/anoxia is partly recorded in the Preafrican Trough, where sediments and bottom waters display slightly dysoxic characteristics in the west (Fig. 10).

During the CCIE, on the Preafrican Trough platform, slightly dysoxic conditions are recorded in the sediments and locally in bottom waters of the deep environments (mid-outer ramp; Fig. 10). In the western part of the Saharan platform (Morocco), dysoxic/anoxic conditions are recorded in the Tarfaya Basin (Sinninghe Damsté and Köster, 1998; Lüning et al., 2004; Keller et al., 2008; Mort et al., 2008), but not in the Agadir Basin (Jati et al., 2010; Lebedel, 2013). Monteiro et al. (2012) show that, during the CCIE, the dysoxic/anoxic conditions reached their maximum extension and were present in the Central and South Atlantic Ocean, Tethys, Pacific and Indian Oceans. However, in very shallow environments, as in the eastern part of the Preafrican Trough platform, the waters remain oxic owing to exchanges with the atmosphere.

The most important disturbances of the late Cenomanian–early Turonian in the western part of the Saharan platform are recorded in the lower Turonian, after the CCIE, where the deposits exhibit the following characteristics. In the Preafrican Trough, thin beds of muddy limestone appear, rich in chert and opportunistic fauna (Lezin et al., 2012; Lebedel et al., 2013). The waters are highly dysoxic and the palaeoproductivity is high (Fig. 10). In the Tarfaya basin, layers rich in organic matter and chert suggest an enhanced palaeoproductivity associated with dysoxic conditions (El Albani et al., 1997; Kuhnt et al., 2004; Lüning et al., 2004). In the Agadir basin, the establishment of black shales and the appearance of abundant opportunistic fauna reflect dysoxic conditions (Terrab, 1994; Jati, 2007; Jati et al., 2010; Lebedel, 2013). In the High Moulouya, the High Atlas, the Middle Atlas and the Essaouira Basin, Ettachfini (2006) highlights sedimentological and palaeontological disturbances similar to those recognized in the Preafrican Trough, linking to the establishment of dysoxic conditions (Lebedel, 2013). In the Guir basin (Southwestern Algeria), the early Turonian facies are similar to those of the Preafrican Trough, with the presence of mudstone, with rare fossils and traces of silicification (Benyoucef and Meister, 2015), which could indicate the installation of dysoxic conditions.

In the Agadir Basin (Terrab, 1994) and the Preafrican Trough platform, the dysoxia continues into the *Nodosoides* Zone, at the end of the early Turonian. In the Tarfaya basin, it seems to persist up to the middle-late Turonian (Aquit et al., 2013). Moreover, the studies of Friedrich et al. (2006), Hetzel et al. (2009) and Van Bentum et al. (2009), on the Demerara rise, show that dysoxic conditions are also developed in the early Turonian, after the CCIE. Thus, in the early Turonian, dysoxic conditions seem to be present in the tropical zone of the Central Atlantic Ocean, as recorded in the upper Cenomanian, before the CCIE (Monteiro et al., 2012).

Other studies are currently in progress to investigate the distribution of Turonian dysoxic conditions. Moreover, the origin of the high palaeoproductivity, as recorded in the Preafrican Trough and the Tarfaya Basin, remains to be explained. Indeed, although the climate was hot and wet on the Preafrican Trough during the early Turonian, another factor may be involved in the establishment of early Turonian dysoxia in the western part of the Saharan platform. This is suggested by the massive presence of silica, the decrease of terrigenous input and the reduction of weatherable continental areas after the 2nd-order Cenomanian transgression, which reflect the probable influence of hydrothermalism and/or volcanism of the Caribbean LIP (Large Igneous Province) and oceanic ridge.

5. Conclusion

The synthesis of data (sedimentological, palaeontological, geochemical, mineralogical, etc.) of the upper Cenomanian–lower Turonian carbonate platform of the Preafrican Trough allows us to propose a 3D model of the platform configuration. In this way, palaeoenvironmental conditions of the Preafrican Trough are compared with those of other platforms at the same period.

During the late Cenomanian and the CCIE (Cenomanian Carbon Isotope Excursion), dysoxic bottom waters are present in the deepest environment of the mid- to outer-ramp, in the west of the platform. In the peritidal to mid-ramp environments of the eastern platform, waters remain well-oxygenated. The climate is arid before the CCIE and warm with contrasted seasons during the CCIE, associated with (1) oligotrophic to mesotrophic palaeoproductivity conditions and (2) the extensive development of a platform mainly composed of photozoan, followed by heterozoan, carbonate-producing ecosystems over a large part of the Saharan platform. However, this scenario is not in accordance with other studies considering that the presence of wet climate during the CCIE, causing an intense chemical weathering of the continents, also leads to an increase of the palaeoproductivity at a global scale. In the Preafrican Trough, the poorly-oxygenated waters spread out from the deep basins and cover the platform in response to sea-level rise.

The most significant event recorded on the platform is early Turonian in age. Just after the Cenomanian/Turonian boundary and the CCIE, the platform is flooded (drowning phase), leading to the development of an outer-ramp environment over the entire platform. This flooding is linked to the end of the major Cenomanian transgression and the establishment of eutrophic conditions which disrupt carbonate-producing organisms. These eutrophic conditions lead to highly dysoxic conditions in the bottom and intermediate waters of the platform, thus leading to the disappearance of the majority of the palaeontological groups, except for opportunist benthic and planktonic foraminifera, which are able to proliferate. The enhanced palaeoproductivity causing the dysoxia is due to increased nutrient inputs. These latter are partly linked to the presence of a hot and wet climate that could induce a slight increase of chemical weathering on the continent. But, the decrease of the detrital influx during the early Turonian, the massive presence of silica and the reduction of weatherable continental areas after the Cenomanian transgression argue for another main source of nutrient input, probably the hydrothermalism/volcanism of the Caribbean LIP and oceanic ridges. The presence of dysoxic/anoxic conditions in several regions of the tropical Central Atlantic during the early Turonian is another argument in favor of this last hypothesis.

Acknowledgements

We gratefully acknowledge C. Cavaré-Hester (GET) for drafting the illustrations. We thank Dr M.S.N. Carpenter for post-editing the English style. The authors are grateful to L. Cavin, the anonymous reviewer and R. Mapeo for improving the manuscript with their critical remarks and suggestions.

Appendix A

Time interval	Samples	Kaolinite (%)	Illite (%)	Smectites (%)	I/S (%)	Palygorskite (%)
Tinghir section						
Before CCIE	T1-1	46.0	38.0	16.0	0.0	0.0
	T3a-1	18.0	10.0	38.0	22.0	12.0
	T4-1	26.0	0.0	24.0	50.0	0.0
	T5	29.0	16.0	17.0	35.0	3.0
	T6-1	11.0	0.0	33.0	56.0	0.0
	T7-1 base	18.0	9.0	25.0	40.0	8.0
	T7-1 top	40.0	0.0	0.0	60.0	0.0
During CCIE	T8c-1	16.5	11.5	32.0	17.5	22.5
	T9-1	19.0	0.0	44.0	37.0	0.0
	T10-1	0.0	0.0	75.0	16.0	9.0
	T12-1	12.0	8.0	15.0	65.0	0.0
After CCIE	T14-1			No clay		
	T14-2	20.0	9.0	11.0	60.0	0.0
	T14-3	21.0	9.0	11.0	59.0	0.0
	T14-4	15.0	0.0	0.0	85.0	0.0
	T15-1	15.0	0.0	0.0	85.0	0.0
	T15-2	17.0	10.0	0.0	73.0	0.0
Izakarène section						
Before CCIE	I1	23.0	25.0	26.0	0.0	26.0
	I3-1	8.0	14.0	34.0	0.0	44.0
	Is5c1	12.0	20.0	20.0	0.0	48.0
During CCIE	I6a-1	20.0	40.0	40.0	0.0	0.0
	I6d	5.0	10.0	37.0	0.0	48.0
	I6i	11.0	13.0	30.0	0.0	46.0
After CCIE	Is86-2	24.0	48.0	0.0	28.0	0.0
	Is96-2	32.0	45.0	0.0	23.0	0.0
	Is100	40.0	47.0	0.0	13.0	0.0
Goulmima section						
Before CCIE	Ga1	6.6	23.3	26.3	35.0	8.8
	Ga4	25.3	29.3	10.7	24.0	10.7
	G0	38.7	21.7	8.5	20.7	10.4
	G1-2	32.4	56.8	0.0	0.0	10.8
During CCIE	G2-2	15.5	33.3	5.9	32.2	13.1
	G3	27.2	42.0	0.0	19.7	11.1
	G5-1	17.2	20.7	9.2	41.4	11.5
	G6	0.0	30.8	12.8	33.3	23.1
	G8	0.0	12.8	41.1	20.5	25.6
	G7b-1	0.0	24.3	28.6	34.3	12.8
	G13	0.0	41.0	18.2	22.6	18.2
	G7d-1			No clay		
	G14	0.0	100.0	0.0	0.0	0.0

Appendix A (*continued*)

Time interval	Samples	Kaolinite (%)	Illite (%)	Smectites (%)	I/S (%)	Palygorskite (%)
After CCIE	G15	0.0	59.5	18.9	21.6	0.0
	G18	0.0	73.7	26.3	0.0	0.0
	G19	0.0	81.8	18.2	0.0	0.0
	G21	0.0	100.0	0.0	0.0	0.0
	G23	0.0	100.0	0.0	0.0	0.0
	G8-10	0.0	100.0	0.0	0.0	0.0
	G8-7	0.0	31.6	50.0	18.4	0.0
	G26	0.0	100.0	0.0	0.0	0.0
	G10-1			No clay		
	G28	0.0	83.8	16.2	0.0	0.0
	G15-1	0.0	100.0	0.0	0.0	0.0

References

Abdallah, H., 2000. L'Evénement anoxique de la limite Cénomanien–Turonien. Thesis, Sciences faculty of Tunis, Tunis II University, 62p.

Aguilera-Franco, N., Romano, U.H., 2004. Cenomanian–Turonian facies succession in the Guerrero-Morelos Basin, Southern Mexico. Sed. Geol. 170, 135–162.

Al-Dulaimi, S.I., Al-Zaidy, A.A., Al-Jumaily, S.S., 2013. The demise stage of rudist bearing Mishrif Formation (late Cenomanian–early Turonian), Southern Iraq. Iraqi Bull. Geol. Min. 9 (3), 1–20.

Andreu, B., 1989. Le Crétacé moyen de la transversale Agadir-Nador (Maroc): précisions stratigraphiques et sédimentologiques. Cretac. Res. 10, 49–80.

Andreu, B., 1991. Les Ostracodes du Crétacé moyen (Barrémien à Turonien), le long d'une transversale Agadir-Nador (Maroc). Strata, Toulouse, France, 756p.

Andreu, B., Lebedel, V., Wallez, M.-J., Lezin, C., Ettachfini, El M., 2013. The upper Cenomanian–lower Turonian carbonate platform of the Preafrican Trough, Morocco: biostratigraphic, palaeoecological and palaeobiogeographical distribution of ostracods. Cretac. Res. 45, 216–246.

Aquit, M., Kuhnt, W., Holbourn, A., Chellai, El H., Stattegger, K., Kluth, O., Jabour, H., 2013. Late Cretaceous paleoenvironmental evolution of the Tarfaya Atlantic costal Basin, SW Morocco. Cretac. Res. 45, 288–305.

Basse, E., Choubert, G., 1959. Les faunes d'ammonites du Cénomano–Turonien de la partie orientale du domaine atlasique marocain et de ses annexes sahariennes. In: Congreso Geologico Internacional. XX Sesion – Ciudad de Mexico, 1956, Symposium del Cretàcico, pp. 59–82.

Benyoucef, M., Adaci, M., Meister, C., Läng, E., Malti, F.-Z., Mebarki, K., Cherif, A., Zaoui, D., Benyoucef, A., Bensalah, M., 2014. Le «Continental Intercalaire» dans la région du Guir (Algérie): nouvelles données paléontologiques, ichnologiques et sédimentologiques. Rev. Paléobiol. 33 (1), 281–297.

Benyoucef, M., Meister, C., 2015. Lithostratigraphic evolution, facies analysis and depositional environment of the Cenomanian lower Turonian in the Guir area, Southwestern Algeria. Cretac. Res. 53, 68–88.

Bomou, B., Adatte, T., Tantawy, A.A., Mort, H., Fleitmann, D., Huang, Y., Föllmi, K.B., 2013. The expression of the Cenomanian–Turonian oceanic anoxic event in Tibet. Palaeogeogr. Palaeoclimatol. Palaeoecol. 369, 466–481.

Caron, M., Robaszynski, F., Amédro, F., Baudin, F., Deconinck, J.-F., Hochuli, P., Von Salis-Perch Nielsen, K., Tribovillard, N., 1999. Estimation de la durée de l'événement anoxique global au passage Cénomanien/Turonien. Approche cyclostratigraphique dans la Formation Bahloul en Tunisie centrale. Bull. Soc. Géol. France 170 (2), 145–160.

Caron, M., Dall' Agnolo, S., Accarie, H., Barrera, E., Kauffman, E.G., Amédro, F., Robaszynski, F., 2006. Stratigraphie à haute résolution de la limite Cénomanien–Turonien sur les coupes de Pueblo (Etats-Unis) et de l'Oued Bahloul (Tunisie): isotopes stables et corrélation des évènements biologiques. Geobios 39, 171–200.

Cavin, L., Tong, H., Boudad, L., Meister, C., Piuz, A., Tabouelle, J., Aarab, M., Amiot, R., Buffetaut, E., Dyke, G., Hua, S., Le Loeuff, J., 2010. Vertebrate assemblages from the early Late Cretaceous of southeastern Morocco: an overview. J. Afr. Earth Sc. 57, 391–412.

Chamley, H., 1989. Clay Sedimentology. Springer-Verlag, pp. 623.

Choubert, G., 1948. Essai sur la paléogéographie du Mésocrétacé marocain. Soc. Sci. Nat., Maroc, 307–329.

Choubert, G., Faure-Muret, A., 1962. Evolution du domaine atlasique marocain depuis les temps paléozoïques. Livre à la mémoire du Professeur Paul Fallot, tome 1. Bull. Soc. Géol. France, Mém. H. S., 447–528

Deconinck, J.F., Chamley, H., Debrabant, P., Colbeaux, J.-P., 1982. Le Boulonnais au Jurassique supérieur: données de la mineralogy des argiles et de la géochmie. Extrait des annales de la Société Géologique du Nord, t. CII, pp. 145–152.

Drzewiecki, P.A., Simo, J.A., 1997. Carbonate platform drowning and oceanic anoxic events on a mid-Cretaceous carbonate platform, south-central Pyrenees, Spain. J. Sedim. Res. 67 (4), 698–714.

Dubar, G., 1948. Notice explicative de la carte géologique provisoire du Haut Atlas de Midelt au 1/200000. Notes et Mémoires du Service géologique, Maroc, 59 bis.

El Albani, A., Caron, M., Deconninck, J.-F., Robaszynski, F., Amedro, F., Daoudi, L., Disnar, J.R., Ezaidid, A., Terrab, S., Thurow, J., 1997. Origines et signification sédimentologique de la nodulisation dans les dépôts anoxiques du Turonien inférieur du Bassin de Tarfaya (Maroc). C.R. Acad. Sci. Paris, t. 324 (serie II a), 9–16.

Elrick, M., Molina-Garza, R., Duncan, R., Snow, L., 2009. C-isotope stratigraphy and paleoenvironmental changes across OAE2 (mid-Cretaceous) from shallow-water platform carbonates of southern Mexico. Earth Planet. Sci. Lett. 277, 295–306.

El-Sabbagh, A., Tantawy, A.A., Keller, G., Khozyemd, H., Spangenberg, J., Adatte, T., Gertsch, B., 2011. Stratigraphy of the Cenomanian–Turonian Oceanic Anoxic Event OAE2 in shallow shelf sequences of NE Egypt. Cretac. Res. 32, 705–722.

El-Shazly, S., Kostak, M., Abdel-Gawad, G., Klouckova, B., Ghanem Saber, S., Felieh Salama, Y., Mazuch, M., Zak, K., 2011. Carbon and oxygen stable isotopes of selected Cenomanian and Turonian rudists from Egypt and Czech Republic, and a note on changes in rudist diversity. Bull. Geosci. 86 (2), 209–226.

Ettachfini, El M., 1993. Le Vraconien, Cénomanien et Turonien du Bassin d'Essaouira (Haut Atlas Occidental). Strata, Toulouse, France, 245p.

Ettachfini, El M., Andreu, B., 2004. Le Cénomanien et le Turonien de la Plate-forme Préafricaine du Maroc. Cretac. Res. 25 (2), 277–302.

Ettachfini, El M., Souhel, A., Andreu, B., Caron, M., 2005. La limite Cénomanien–Turonien dans le Haut Atlas central, Maroc. Geobios 38, 57–68.

Ettachfini, El M., 2006. La transgression au passage du Cénomanien au Turonien sur le domaine atlasique marocain. Stratigraphie intégrée et relation avec l'évenement océanique global. Ph.D. Thesis, Chouaïb Doukkali University, El Jadida, Strata 2, 45, 299p.

Faouzi Zagrarni, M.F., HédiNegra, M., Hanini, A., 2008. Cenomanian–Turonian facies and sequence stratigraphy, Bahloul Formation, Tunisia. Sed. Geol. 204, 18–35.

Flögel, S., Wallmann, K., Poulsen, C.J., Zhou, J., Oschlies, A., Voigt, S., Kuhnt, W., 2011. Simulating the biogeochemical effects of volcanic CO_2 degassing on the oxygen-state of the deep ocean during the Cenomanian/Turonian Anoxic Event (OAE2). Earth Planet. Sci. Lett. 305, 371–384.

Föllmi, K.B., Weissert, H., Bisping, M., Funk, H., 1994. Phosphogenesis, carbon-isotope stratigraphy, and carbonate-platform evolution along the Lower Cretaceous northern Tethyan margin. Am. Assoc. Petrol. Geol., Bull. 106, 729–746.

Friedrich, O., Erbacher, J., Mutterlose, J., 2006. Paleoenvironmental changes across the Cenomanian/Turonian Boundary Event (Oceanic Anoxic Event 2) as indicated by benthic foraminifera from the Demerara Rise (ODP Leg 207). Rev. Micropaléontol. 49, 121–139.

Friedrich, O., 2010. Benthic foraminifera and their role to decipher paleoenvironment during mid-Cretaceous Oceanic Anoxic Events – the "anoxic benthic foraminifera" paradox. Revue Micropaleontol. 53, 175–192.

Friedrich, O., Norris, R.D., Erbacher, J., 2011. Evolution of middle to Late Cretaceous oceans – A 55 m.y. record of Earth's temperature and carbon cycle. Geol. Soc. Am. 40 (2), 107–110.

Gale, A.S., Jenkyns, H.C., Kennedy, W.J., Corfield, R.M., 1993. Chemostratigraphy versus biostratigraphy data from around the Cenomanian–Turonian boundary. J. Geol. Soc. Lond. 150, 29–32.

Gale, A.S., Kennedy, W.J., Voigt, S., Walaszczyk, I., 2005. Stratigraphy of the Upper Cenomanian–Lower Turonian Chalk succession at Eastbourne, Sussex, UK: ammonites, inoceramid bivalves and stable carbon isotopes. Cretac. Res. 26, 460–487.

Gebhardt, H., Friedrich, O., Schenk, B., Fox, L., Hart, M., Wagreich, M., 2010. Paleoceanographic changes at the northern Tethyan margin during the Cenomanian–Turonian Oceanic Anoxic Event (OAE-2). Mar. Micropaleontol. 77, 25–45.

Gertsch, B., Adatte, T., Keller, G., Tantawy, A.A.A.M., Berner, Z., Mort, H.P., Fleitmann, D., 2010a. Middle to late Cenomanian oceanic anoxic event in shallow and deeper shelf environments of western Morocco. Sedimentology 57 (6), 1430–1462.

Gertsch, B., Keller, G., Adatte, T., Berner, Z., Kassab, A.S., Tantawy, A.A.A., El-Sabbagh, A.M., Stueben, D., 2010b. Cenomanian–Turonian transition in a shallow water sequence of the Sinai, Egypt. Int. J. Earth Sci. 99 (1), 165–182.

Grosheny, D., Chikhi-Aouimeur, F., Ferry, S., Benkherouf-Kechid, F., Jati, M., Atrops, F., Redjimi-Bourouiba, W., 2008. The Upper Cenomanian–Turonian (Upper Cretaceous) of the Saharan Atlas (Algeria). Bull. Soc. Géol. Fr. 179 (6), 593–603.

Grosheny, D., Ferry, S., Jati, M., Ouaja, M., Bensalah, M., Atrops, F., Chikhi-Aouimeur, F., Benkerouf-Kechid, F., Negra, H., Aït Salem, H., 2013. The Cenomanian–Turonian boundary on the Saharan Platform (Tunisia and Algeria). Cretac. Res. 42, 66–84.

Hardenbol, J., Thierry, J., Farley, M.B., Jacquin, T., De Granciansky, P.-C., Vail, P.R., 1998. Mesozoic and Cenozoic Sequence Chronostratigraphic Framework of European Basins. In: De Graciansky, P.-C., Hardenbol, J., Jacquin, T., Vail, P.R., (Eds.), Mesozoic and Cenozoic Sequence Stratigraphy of European Basins, SEPM Special Publication 60.

Herkat, M., 1999. La sédimentation de haut niveau marin du Crétacé supérieur de l'Atlas saharien oriental et des Aurès. Stratigraphie séquentielle. Analyse quantitative des biocénoses, évolution paléogéographique et contexte géodynamique. Ph.D. Thesis, USTHB University, Alger.

Herkat, M., 2004. Contrôle eustatique et paléogéographique de la sédimentation du Crétacé supérieur du bassin des Aurès (Algérie). Bull. Soc. Géol. Fr. 175 (3), 273–288.

Hernàndez-Romano, U., Aguilera-Franco, N., Martinez-Medrano, M., Barcelo-Duarte, J., 1997. Guerrero-Morelos Platform drowning at the Cenomanian–Turonian boundary, Huitziltepec area, Guerrero State, southern Mexico. Cretac. Res. 18, 661–686.

Hetzel, A., Böttcher, M.E., Wortmann, U.G., Brumsack, H.J., 2009. Paleo-redox conditions during OAE2 reflected in Demerara Rise sediment geochemistry (ODP Leg 207). Palaeogeogr. Palaeoclimatol. Palaeoecol. 273, 302–328.

Jarvis, I., Lignum, J.S., Gröcke, D.R., Jenkyns, H.C., Pearce, M.A., 2011. Black shale deposition, atmospheric CO_2 drawdown, and cooling during the Cenomanian–Turonian Oceanic Anoxic Event. Paleoceanography 26, 17.

Jati, M., 2007. Le passage Cénomanien–Turonien du continent nord africain (Maroc, Algérie, Tunisie). Comparaison avec le bassin subalpin: apport de la sédimentologie et de la géochimie isotopique. Ph.D. Thesis, Louis Pasteur Univ., Strasbourg I, 247p.

Jati, M., Grosheny, D., Ferry, S., Masrour, M., Aoutemc, M., Içame, N., Gauthier-Lafaye, F., Desmares, D., 2010. The Cenomanian–Turonian boundary event on the Moroccan Atlantic margin (Agadir basin): stable isotope and sequence stratigraphy. Palaeogeogr. Palaeoclimatol. Palaeoecol. 296, 151–164.

Jenkyns, H.C., 1991. Impact of Cretaceous sea level rise and anoxic events on the Mesozoic carbonate platform of Yugoslavia. Am. Assoc. Pet. Geol. Bull. 75, 1007–1017.

Jenkyns, H.C., Forster, A., Schouten, S., Sinninghe Damsté, J.S., 2004. High temperatures in the Late Cretaceous Arctic Ocean. Nature 432, 888–892.

Jenkyns, H.C., 2010. Geochemistry of oceanic anoxic events. Geochem. Geophys. Geosyst. 11, 30.

Keller, G., Adatte, T., Berner, Z., Chellai, E.H., Stueben, D., 2008. Oceanic events and biotic effects of the Cenomanian–Turonian anoxic event, Tarfaya Basin, Morocco. Cretac. Res. 29, 976–994.

Kennedy, W.J., Gale, A.S., Ward, D.J., Underwood, C.J., 2008. Early Turonian ammonites from Goulmima, southern Morocco. Bull. de l'institut Royal des Sci. Nat. de Belg., Sci. de la Terre 78, 149–177.

Koutsoukos, E.A.M., Leary, P.N., Hart, M.B., 1990. Latest Cenomanian–earliest Turonian low-oxygen tolerant benthonic foraminifera: a case-study from the Sergipe basin (N.E. Brazil) and the western Anglo-Paris basin (southern England). Palaeogeogr. Palaeoclimatol. Palaeoecol. 77, 145–177.

Kuhnt, W., Herbin, J.P., Thurow, J., Wiedmann, J., 1990. Distribution of Cenomanian–Turonian Organic facies in the Western Mediterranean and along the Adjacent Atlantic Margin. In: HUC A. Y., (Ed.), Deposition of Organic Facies. AAPG Studies in Geology, vol. 30, pp. 133–160.

Kuhnt, W., Luderer, F., Nederbragt, S., Thurow, J., Wagner, T., 2004. Orbital-scale record of the late Cenomanian–Turonian oceanic anoxic event (OAE-2) in the Tarfaya Basin (Morocco). Int. J. Earth Sci. (GeolRundsch) 94, 147–159.

Lebedel, V., Lezin, C., Andreu, B., Wallez, M.-J., Ettachfini, El M., Riquier, L., 2013. Geochemical and palaeoecological record of the Cenomanian–Turonian Anoxic Event in the carbonate platform of the Preafrican Trough, Morocco. Palaeogeogr. Palaeoclimatol. Palaeoecol. 369, 79–98.

Lebedel, V., 2013. Enregistrement de l'èvènement anoxique Cénomanien supérieur–Turonien inférieur à l'ouest de la plate-forme saharienne. PhD thesis, Toulouse University, 323p.

Lezin, C., Andreu, B., Ettachfini, El M., Wallez, M.-J., Lebedel, V., Meister, C., 2012. The Upper Cenomanian–lower Turonian of the Preafrican Trough, Morocco. Sed. Geol. 245–246, 1–16.

Lüning, S., Kolonic, S., Belhadj, Z., Cota, L., Baric, G., Wagner, T., 2004. Integrated depositional model for the Cenomanian–Turonian organic-rich strata in North Africa. Earth-Sci. 64, 51–117.

Ly, A., Kuhnt, W., 1994. Late Cretaceous benthic foraminiferal assemblages of the Casamance shelf (Senegal, NW Africa). Indication of late Cretaceous oxygen minimum zone. Revue Micropaléontol. 37 (1), 49–74.

Meister, C., Rhalmi, M., 2002. Quelques ammonites du Cénomanien–Turonien de la région d'Errachidia-Boudnind-Erfoud (partie méridionale du Haut Atlas central, Maroc). Revue Paléobiol. Genève 21 (2), 759–779.

Meister, C., Piuz, A., 2013. Late Cenomaniane–Early Turonian ammonites of the southern Tethys margin from Morocco to Oman: biostratigraphy, paleobiogeography and morphology. Cretac. Res. 44, 83–103.

Monteiro, F.M., Pancost, R.D., Ridgwell, A., Donnadieu, Y., 2012. Nutrients as the dominant control on the spread of anoxia and euxinia across the Cenomanian–Turonian oceanic anoxic event (OAE2): model-data comparison. Paleoceanography 27, 1–17.

Mort, H., Adatte, T., Föllmi, K.B., Keller, G., Steinmann, P., Matera, V., Berner, Z., Stüben, D., 2007. Phosphorus and the roles of productivity and nutrient recycling during oceanic anoxic event 2. Geology 35 (6), 483–486.

Mort, H., Adatte, T., Keller, G., Bartels, D., Föllmi, K., Steinmann, P., Berner, Z., Chellai, E.H., 2008. Organic carbon deposition and phosphorus accumulation during Oceanic Anoxic Event 2 in Tarfaya. Morocco. Cretac. Res. 29, 1008–1023.

Nederbragt, A.J., Fiorentino, A., 1999. Stratigraphy and palaeoceanography of the Cenomanian–Turonian Boundary Event in Oued Mellegue, north-western Tunisia. Cretac. Res. 20, 47–62.

Parente, M., Frijia, G., Di Lucia, M., 2007. Carbon-isotope stratigraphy of Cenomanian–Turonian platform carbonates from the southern Appennines (Italy): a chemostratigraphic approach to the problem of correlation between shallow-water and deep-water successions. J. Geol. Soc., Lond. 164, 609–620.

Parente, M., Frijia, G., Di Lucia, M., Jenkyns, H.C., Woodfine, R.G., Baroncini, F., 2008. Stepwise extinction of larger foraminifers at the Cenomanian–Turonian boundary: a shallow-water perspective on nutrient fluctuations during Oceanic Anoxic Event 2 (Bonarelli Event). Geology 36 (7), 715–718.

Philip, J., Airaud-Crumiere, C.A., 1991. The demise of the rudist-bearing carbonate platforms at the Cenomanian/Turonian boundary: a global control. Coral Reefs 10, 115–125.

Philip, J., Borgomano, J., Al-Maskiry, S., 1995. Cenomanian–early Turonian carbonate platform of Northern Oman: stratigraphy and palaeo-environments. Palaeogeogr. Palaeoclimatol. Palaeoecol. 119, 77–92.

Robaszynski, F., Caron, M., Dupuis, C., Amédro, F., Gonzalez-Donozo, J.M., Linares-Rodriguez, D., Hardenbol, J., Gartner, S., Calandra, F., Deloffre, R., 1990. A tentative integrated stratigraphy in the Turonian of central Tunisia: formations, zones and sequential stratigraphy in the Kalaat Senan area. Bull. Centres Rech. Explor. – Prod. Elf-Aquit. 14 (1), 213–384.

Sageman, B.B., Meyers, S.R., Arthur, M.A., 2006. Orbital time scale and new C-isotope record for Cenomanian–Turonian boundary stratotype. Geology 34 (2), 125–128.

Schlanger, S.O., Arthur, M.A., Jenkyns, H.C., Scholle, P.A., 1987. The Cenomanian–Turonian oceanic anoxic event, I. Stratigraphy and distribution of organic carbon-rich beds and the marine $\delta^{13}C$ excursion. In: Brooks, J., Fleet, A.J. (Eds.), Marine Petroleum Source Rocks, Geological Society Special Publication 26. Blackwell, Oxford, UK, pp. 371–399.

Schulze, F., 2003. Growth and Crises of the Late Albian–Turonian Carbonate Plateform, West Central Jordan: Integrate Stratigraphy and Environmental Changes. PhD thesis at the Bremen University, Germany, 166p.

Schulze, F., Kuss, J., Marzouk, A., 2005. Platform configuration, microfacies and cyclicities of the upper Albian to Turonian of west-central Jordan. Facies 50, 505–527.

Sereno, P.C., Dutheil, D.B., Larochene, M., Larsson, H.C.E., Lyon, G.H., Magwene, P.M., Sidor, C.A., Varricchio, D.J., Wilson, J.A., 1996. Predatory Dinosaurs from the Sahara and Late Cretaceous Faunal differentiation. Sci., New Serie 272 (5264), 986–991.

Sinninghe Damsté, J.S., Köster, J., 1998. A euxinic southern North Atlantic Ocean during the Cenomanian/Turonian oceanic anoxic event. Earth Planet. Sci. Lett. 158, 165–173.

Sinninghe Damsté, J.S., Kuypers, M.M.M., Pancost, R.D., Schouten, S., 2008. The carbon isotopic response of algae, (cyano)bacteria, archaea and higher plants to the late Cenomanian perturbation of the global carbon cycle: insights from biomarkers in black shales from the Cape Verde Basin (DSDP Site 367). Org. Geochem. 39, 1703–1718.

Steuber, T., Rauch, M., Masse, J.P., Graaf, J., Malkoc, M., 2005. Low-latitude seasonality of Cretaceous temperatures in warm and cold episodes. Nature 437, 1341–1344.

Terrab, S., 1994. Le Cénomanien–Turonien d'Agadir. Stratigraphie et diagénèse (nodulisation). Ph.D. Thesis, Ecole Nationale Supérieure des Mines de Paris, 248p.

Thiry, M., Pletsch, T., 2011. Palygorskite Clays in Marine Sediments: Records of Extreme Climate. In: Galán, E., Singer, A., (Eds.), Developments in Palygorskite-Sepiolite Research. Developments in Clay Science, Vol. 3. Elsevier (Amsterdam), pp. 101–124.

Trabucho Alexandre, J., Tuenter, E., Henstra, G.A., Van der Zwan, K.J., Van de Wal, R.S.W., Dijkstra, H.A., De Boer, P.L., 2010. The mid-Cretaceous North Atlantic nutrient trap: black shales and OAEs. Paleoceanography 25, PA4201.

Tsikos, H., Jenkyns, H.C., Walsworth-Bell, B., Forster, A., Kolonic, S., Erba, E., Premolisilva, I., Baas, M., Wagner, T., Sinninghedamste, J.S., 2004. Carbon-isotope stratigraphy recorded by the Cenomanian–Turonian Oceanic Anoxic Event: correlation and implications based on three key localities. J. Geol. Soc., Lond. 161, 711–719.

Van Bentum, E.C., Hetzel, A., Brumsack, H.-J., Forster, A., Reichart, G.J., Sinninghe Damsté, J.S., 2009. Reconstruction of water column anoxia in the equatorial Atlantic during the Cenomanian–Turonian oceanic anoxic event using biomarker and trace metal proxies. Palaeogeogr. Palaeoclimatol. Palaeoecol. 280, 489–498.

Van Bentum, E.C., Reichart, G.-J., Forster, A., Sinninghe Damsté, J.S., 2012. Latitudinal differences in the amplitude of the OAE-2 carbon isotopic excursion: pCO_2 and paleo productivity. Biogeosciences 9, 717–731.

Voigt, S., Hay, W.W., Höfling, R., DeConto, R.M., 1999. Biogeographic distribution of late Early to Late Cretaceous rudist-reef in the Mediterranean as climate indicator. Geol. Soc. Am. Special Paper 332, 91–103.

Voigt, S., Gale, A.S., Flögel, S., 2004. Midlatitude shelf seas in the Cenomanian–Turonian greenhouse world: temperature evolution and North Atlantic circulation. Palaeoceanography 19, 17.

Westermann, S., Caron, M., Fiet, N., Fleitmann, D., Matera, V., Adatte, T., Föllmi, K.B., 2010. Evidence for oxic conditions during oceanic anoxic event 2 in the northern Tethyan pelagic realm. Cretac. Res. 31, 500–514.

Wilmsen, M., Niebuhr, B., Chellouche, P., Pürner, T., Kling, M., 2010. Facies pattern and sea-level dynamics of the early Late Cretaceous transgression: a case study from the lower Danubian Cretaceous Group (Bavaria, southern Germany). Facies 56, 483–507.